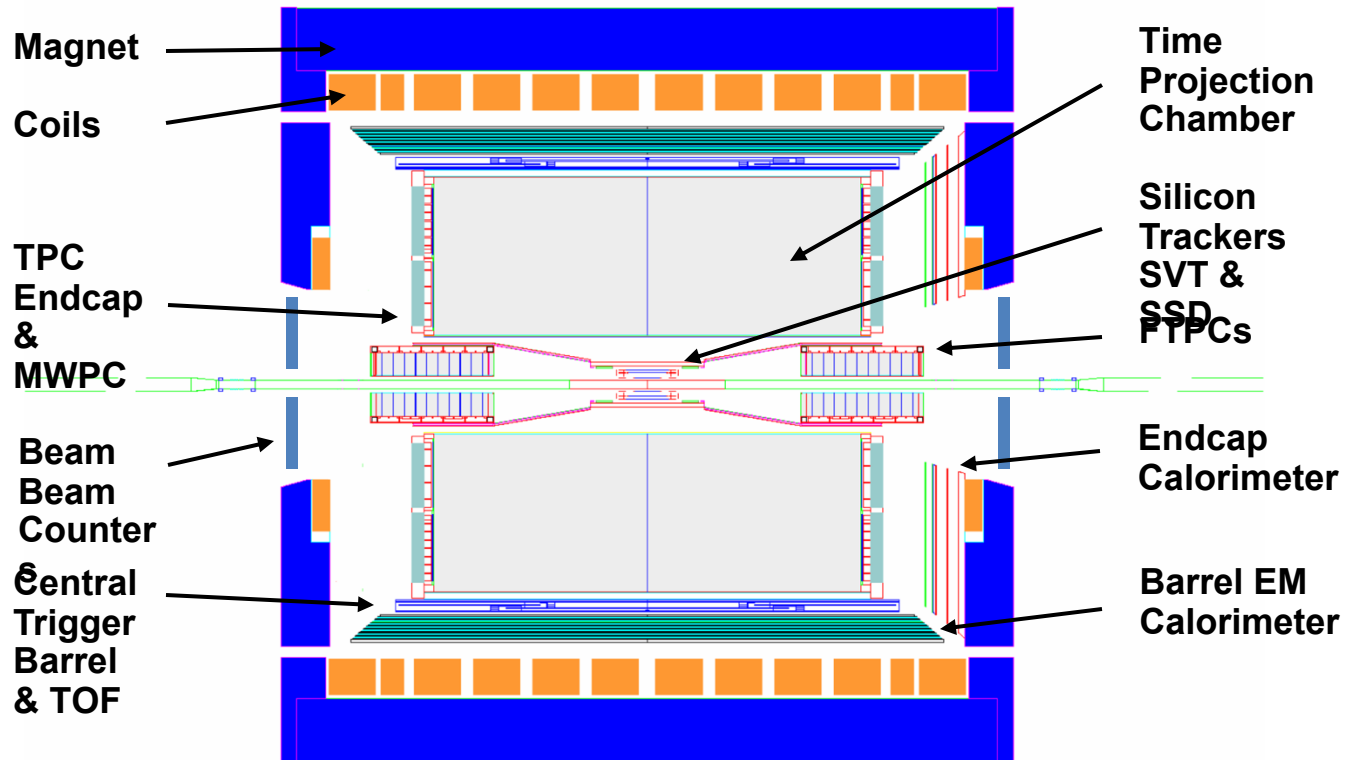


STAR
Time projection Chamber
and
Heavy Flavor Tracker (HFT)

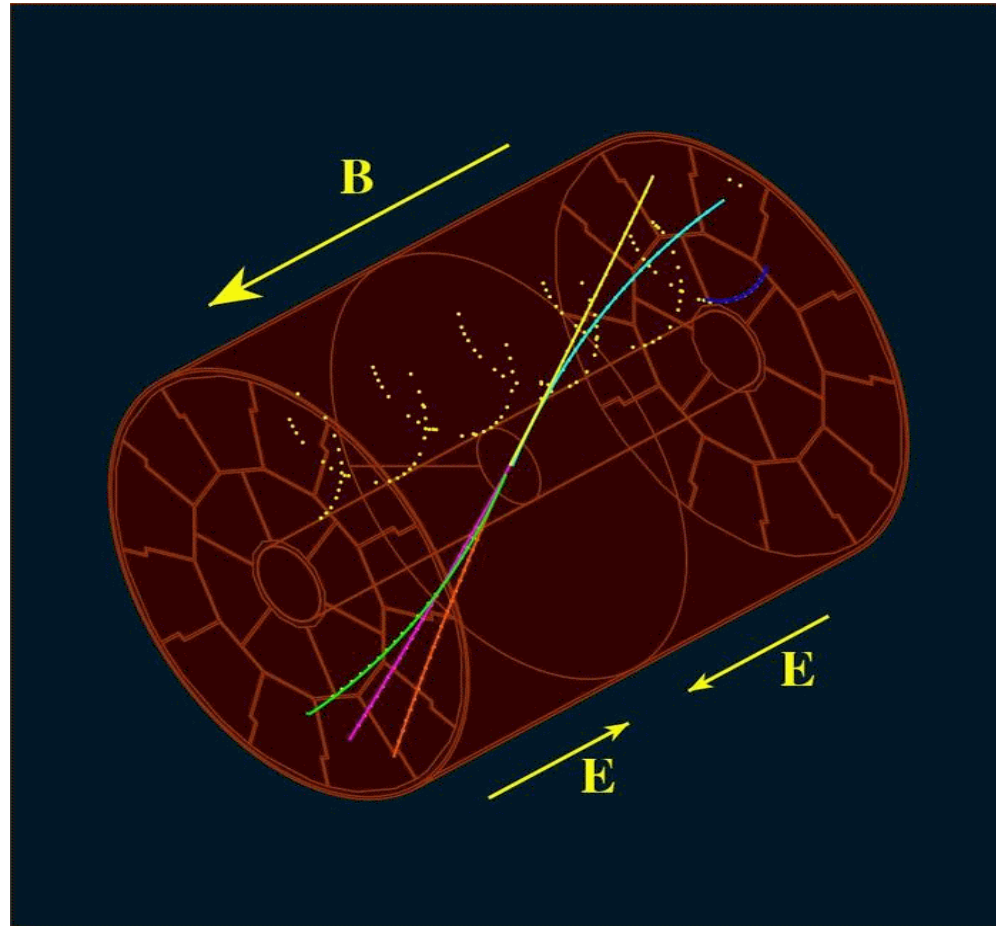
Flemming Videbæk
Brookhaven National Lab

The STAR Detector at RHIC

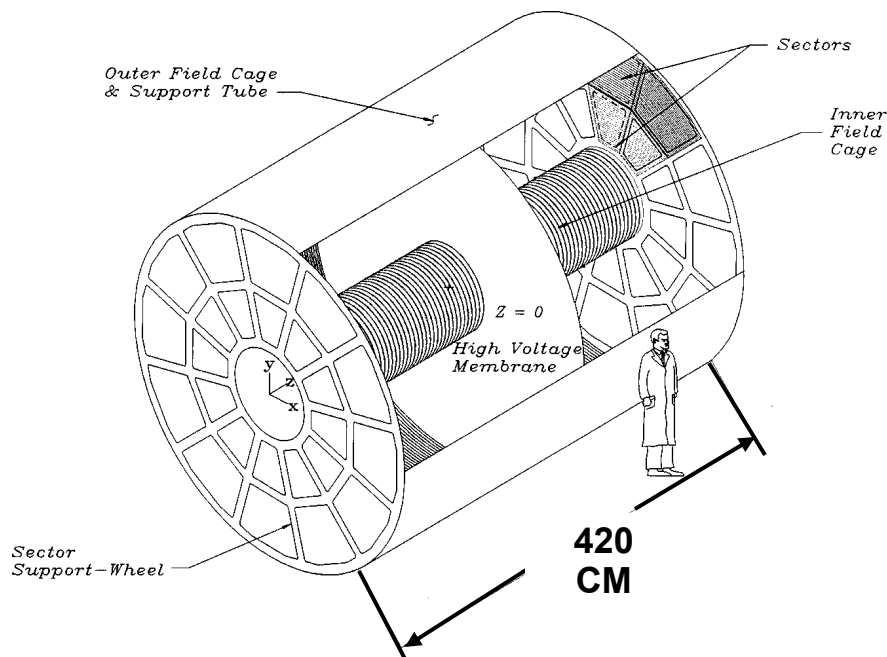


The central STAR detector with the TPC is the key element of STAR

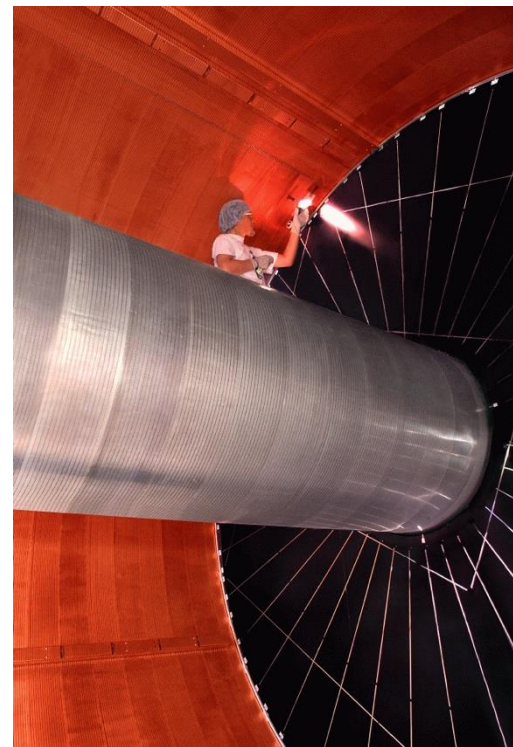
Principles of TPC Operation



TPC: Principles of Operation



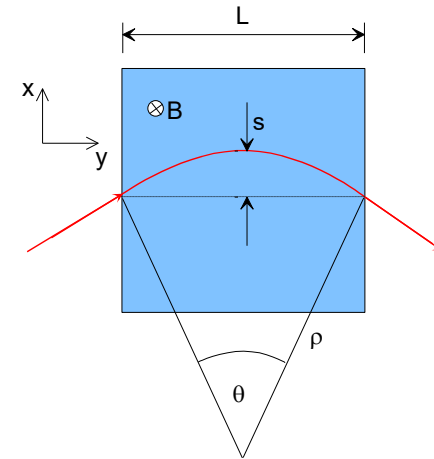
- **Voltage :** - 28 kV at the central membrane
135 V/cm over 210 cm drift path



Secondary electrons, resulting from a primary track, drift in parallel and uniform electric and magnetic fields inside the TPC. These electrons are 'captured' as a function of time by a 2D readout system on the endcaps to form a 3D image.

The STAR Magnet

(room temperature Aluminum coils)



A charged particle in a uniform field follows a (perfect) circular path

$$m \frac{d\vec{v}}{dt} = q (\vec{v} \times \vec{B}) \rightarrow \frac{m v^2}{\rho} = q |\vec{v} \times \vec{B}|$$

$$\frac{m v^2}{\rho} = q |\vec{v} \times \vec{B}| \rightarrow p_T = q B \rho$$

$$p_T \text{ (GeV/c)} = 0.3 B \rho \text{ (T} \cdot \text{m)}$$

3D: The Time Projection Chamber

Time Projection Chamber → full 3-D track reconstruction **STAR TPC**

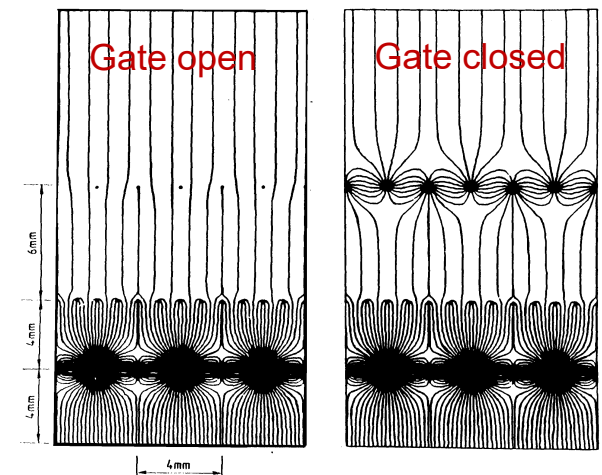
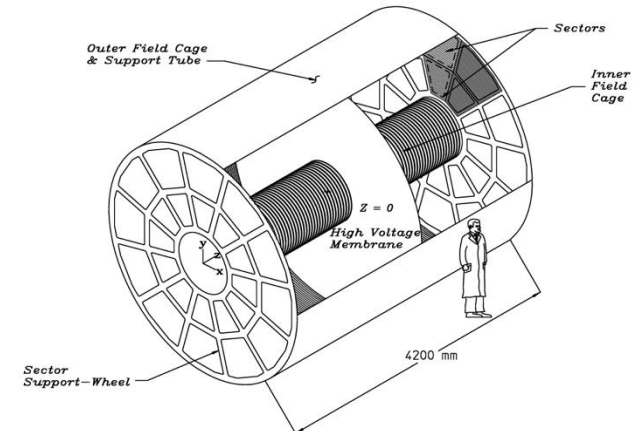
- x-y from wires and segmented cathode of MWPC
- z from drift time
- in addition dE/dx information (charge of ionization)

Diffusion significantly reduced by B-field.

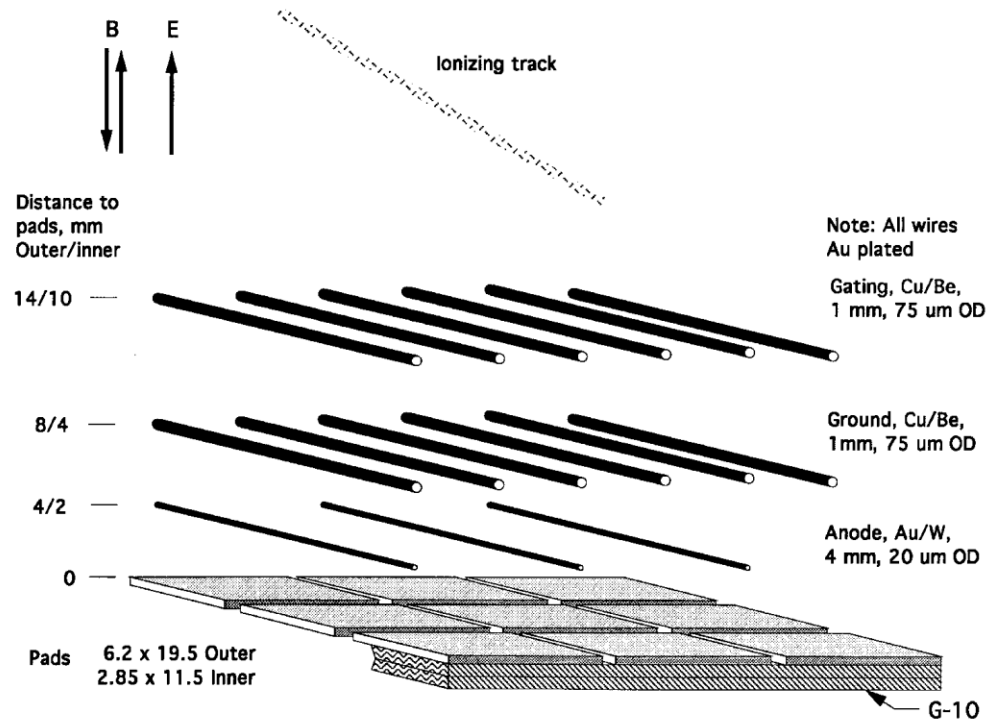
Requires precise knowledge of v_D → LASER calibration + p,T corrections

Drift over long distances → very good gas quality required

Space charge problem from positive ions, drifting back to central membrane → use a gated grid



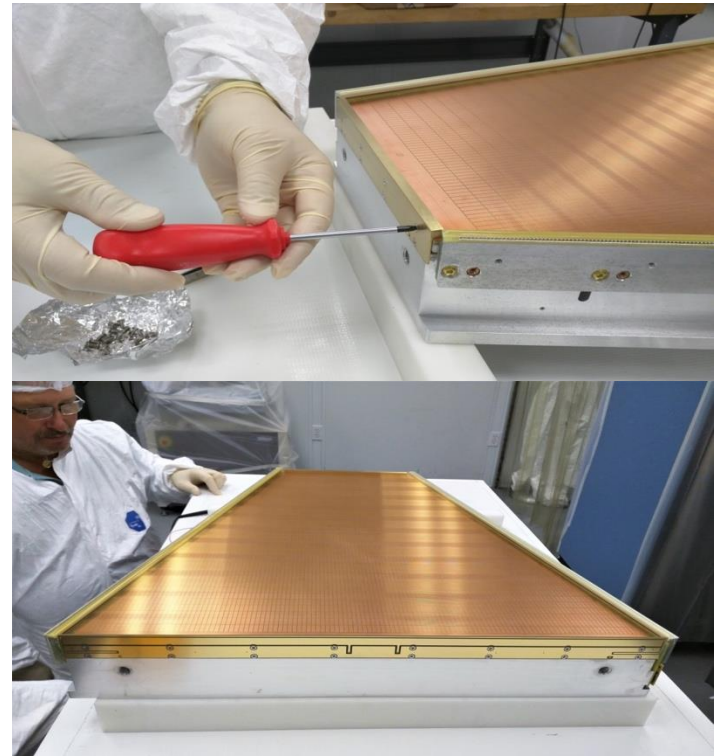
Sector Wire Geometry



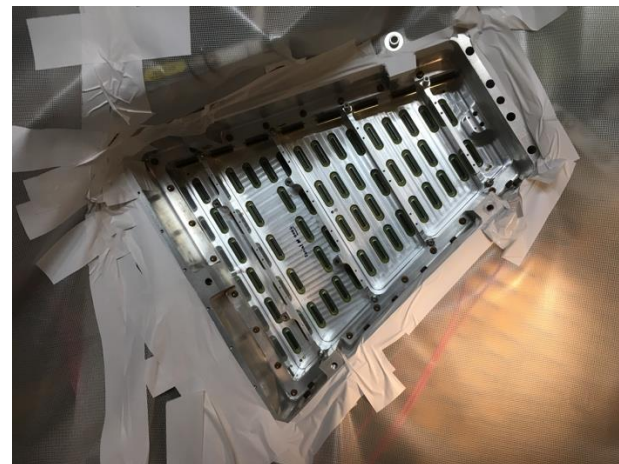
Blown up picture of sensitive area on readout chambers

Picture of Chambers and pad plane (iTPC)

- The STAR TPC was upgraded in 2019 with improved chambers that increased acceptance and accuracy (Beam Energy Scan)
- Here pad plane and wire planes during final assembly



Actual installation



Electronics

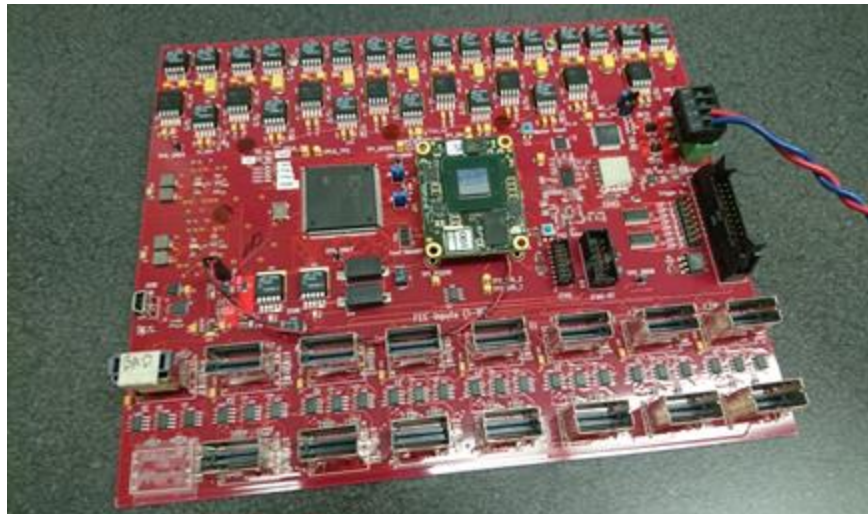
- Doubling #channels per FEE card. 2 SAMPA per FEE
- 55 FEEs per inner sector
- 16 FEEs per RD0
- 4 RDOs per inner sector



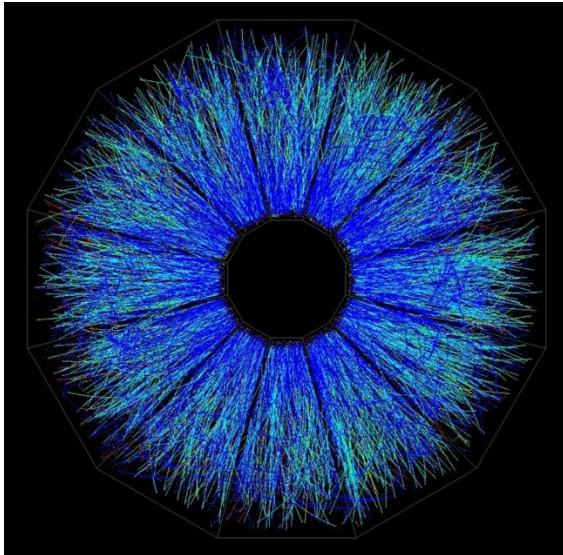
iFFE

Pre-production RDO-- installed

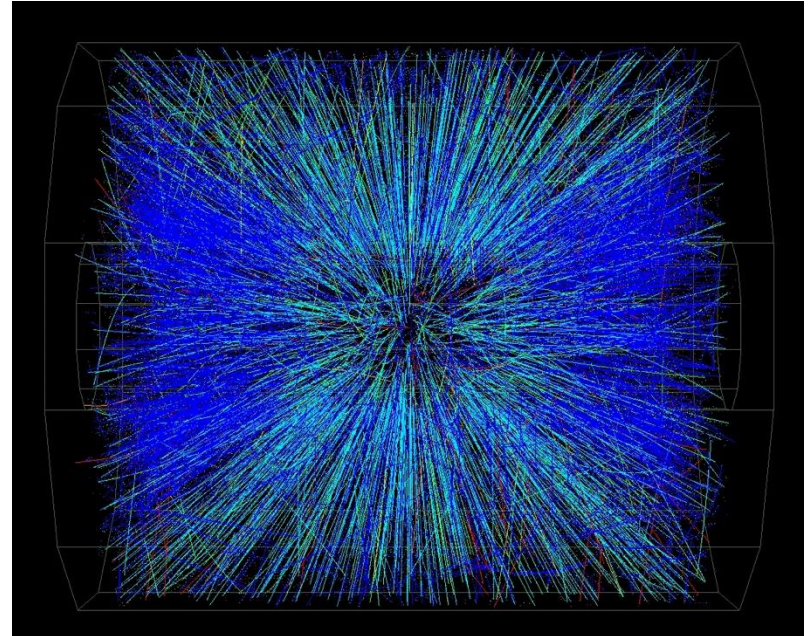
Readout
Board



Au on Au Event at CM Energy ~ 130 GeV*A



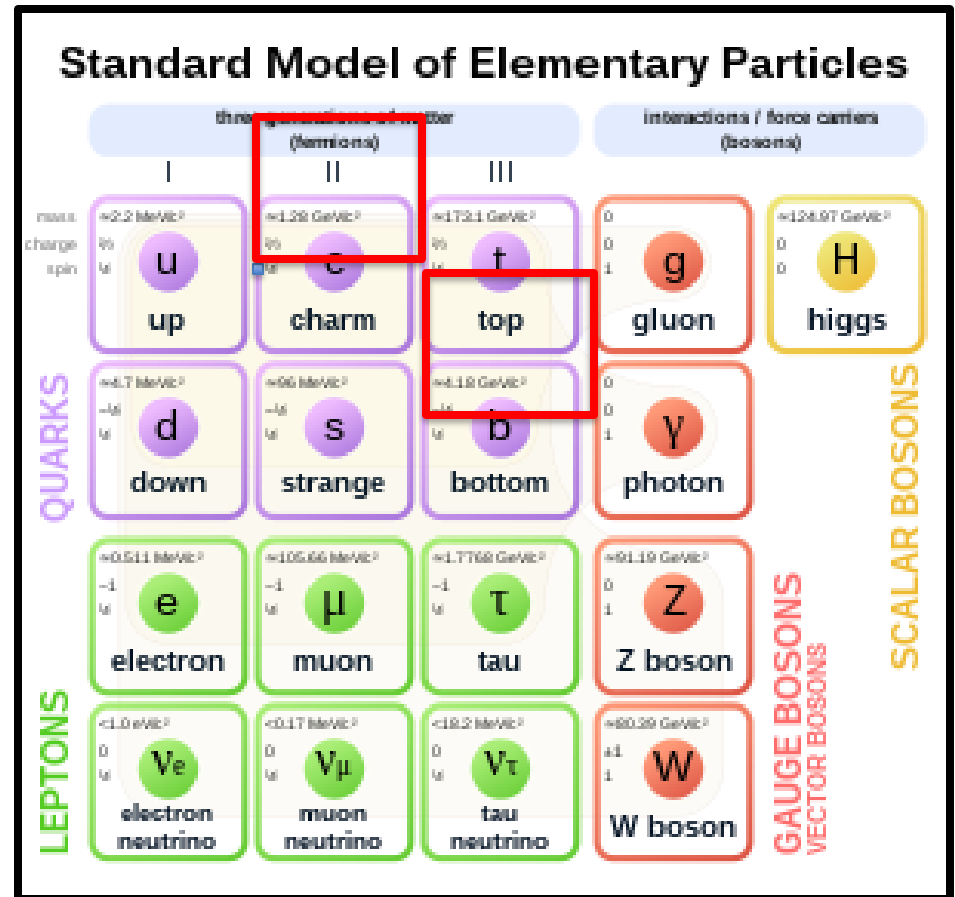
Data Taken June 25,
2000.



Physics Goal

Heavy Flavor

- Heavy quarks at RHIC
- Charm $M \sim 1280 \text{ MeV}$
- Bottom/beauty $M \sim 4180 \text{ MeV}$
- Heavy quarks usually created in pairs $c, c\text{-bar}$ $b, b\text{-bar}$
- Forms mesons, baryons that decays rather quickly with few mm.



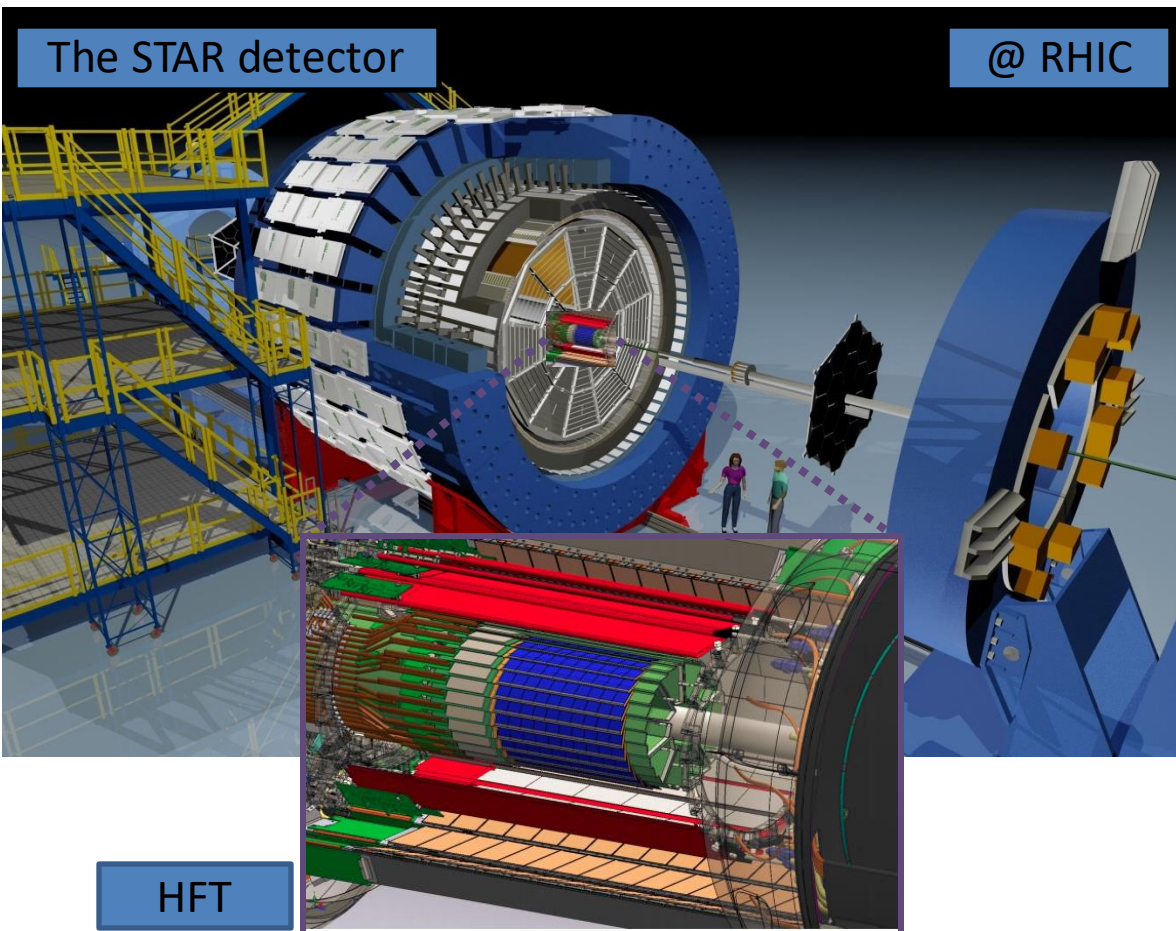
STAR HFT Physics Motivation

Extend the measurement capabilities in the *heavy flavor* domain, good probe to QGP:

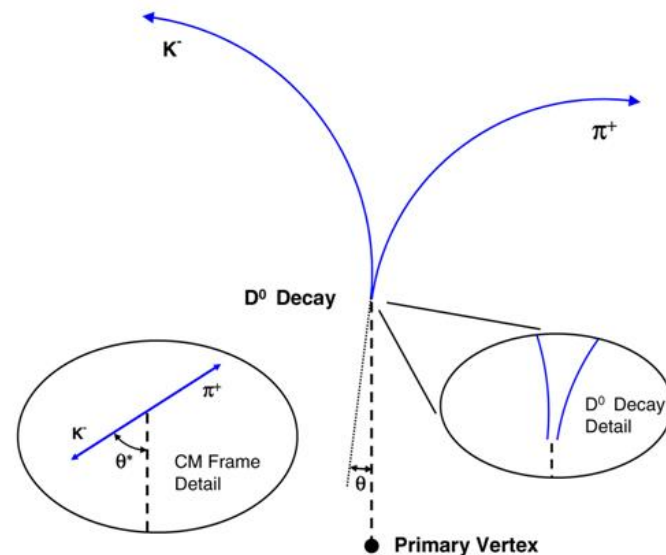
- Direct topological reconstruction of charm hadrons (small $c\tau$ decays, e.g. $D^0 \rightarrow K \pi$)

The STAR detector

@ RHIC



HFT



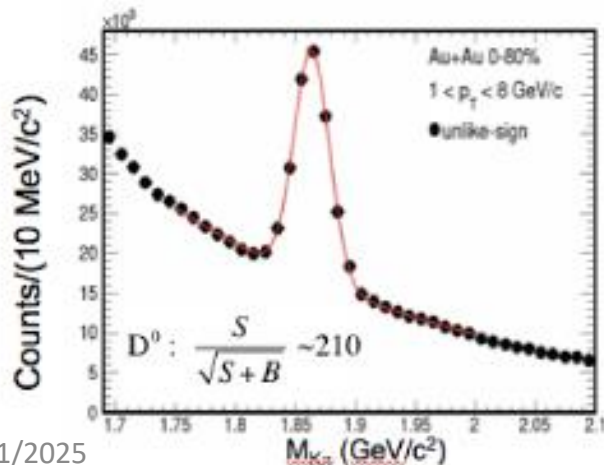
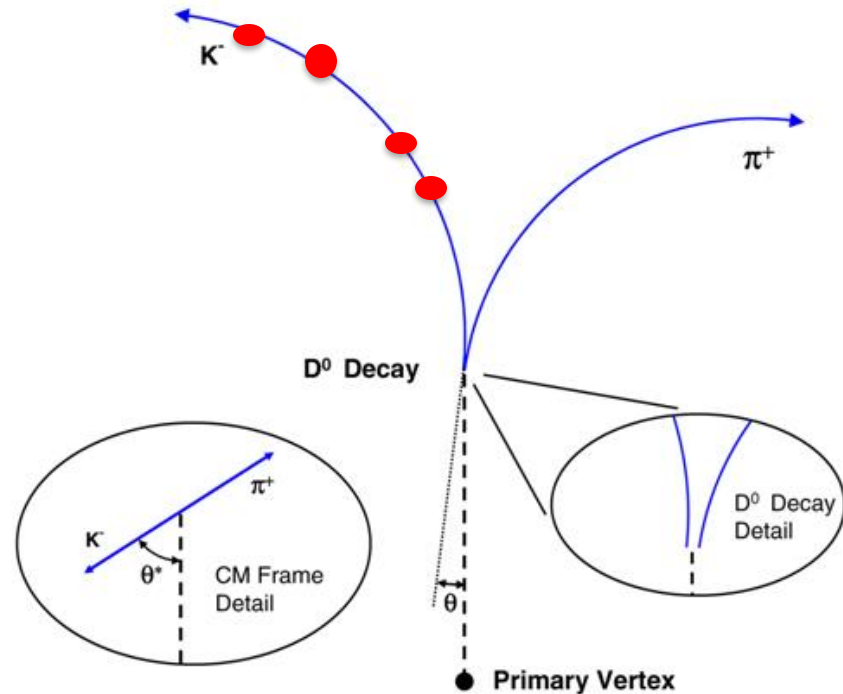
Method: Resolve displaced vertices
($\sim 120 \mu\text{m}$)

200 GeV Au+Au collisions @ RHIC

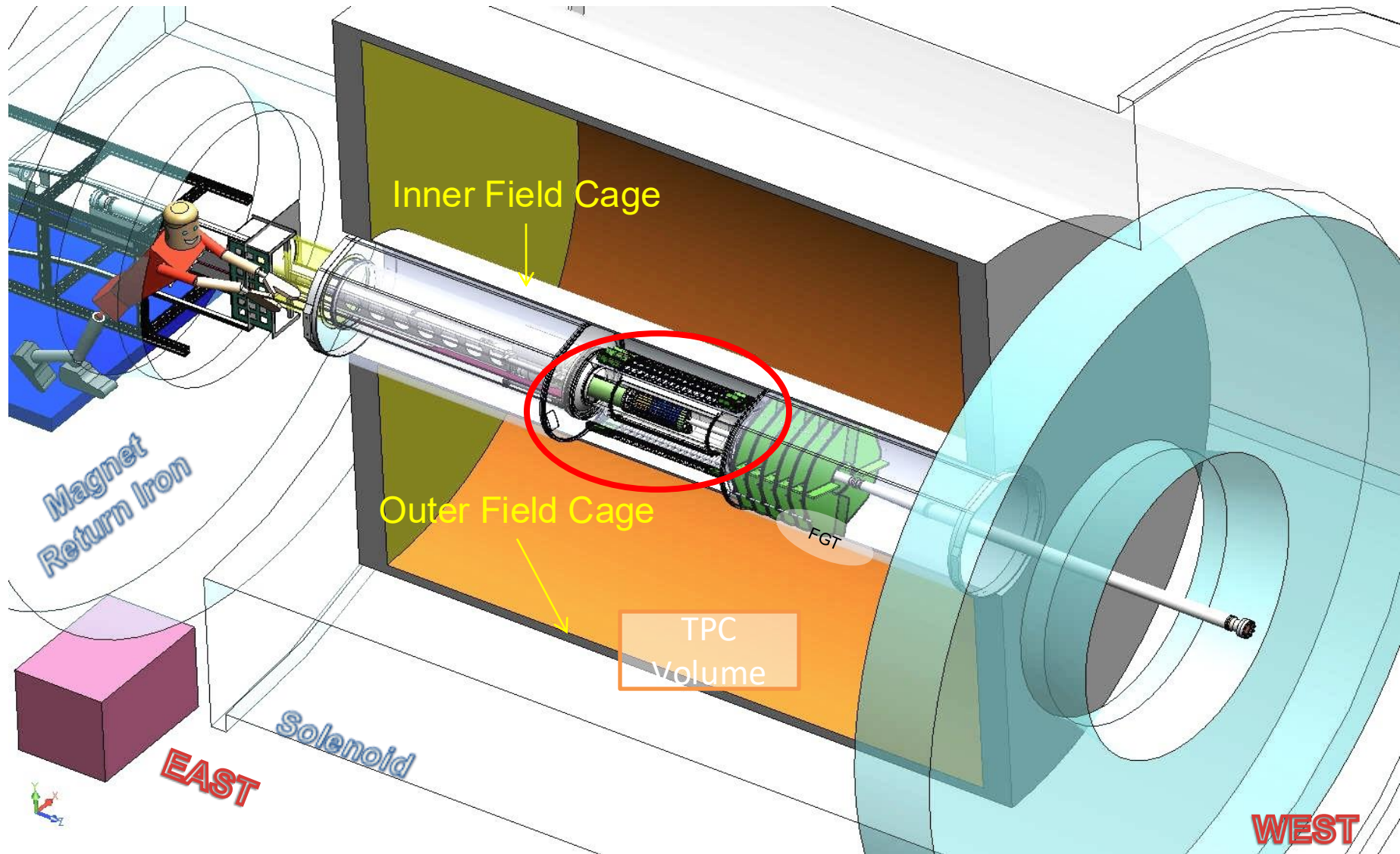
► $dN_{ch}/d\eta \sim 700$ in central events

How are measurements done?

- Measure points on the tracks
- Determine momentum by fitting to a circle (helix)
- Project to primary vertex,
- Determine decay point and angles.
- From the momenta and masses of decay products calculate mass of decaying meson



Heavy Flavor Tracker (HFT)



HFT was installed into STAR

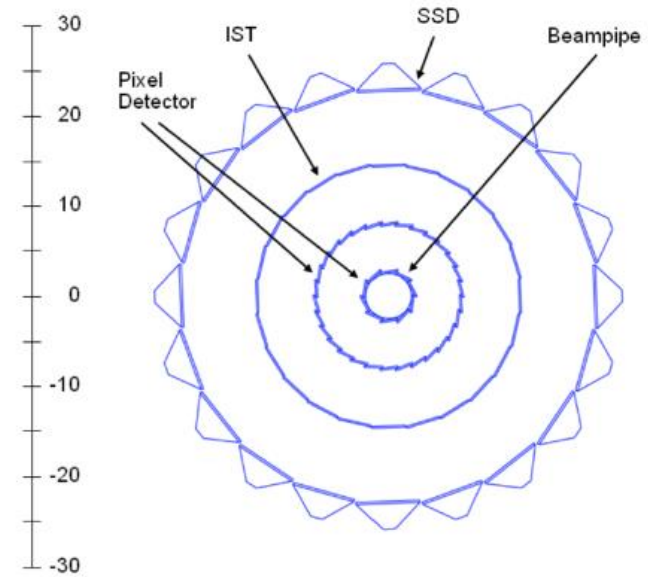
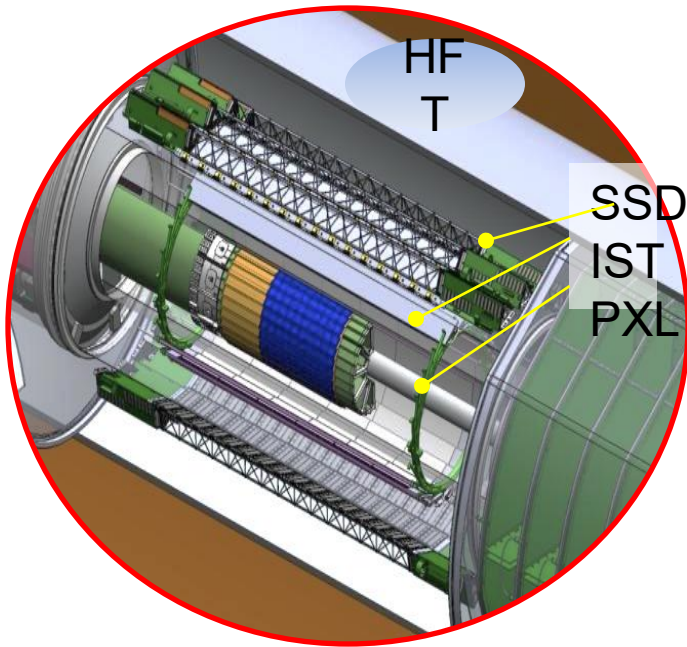
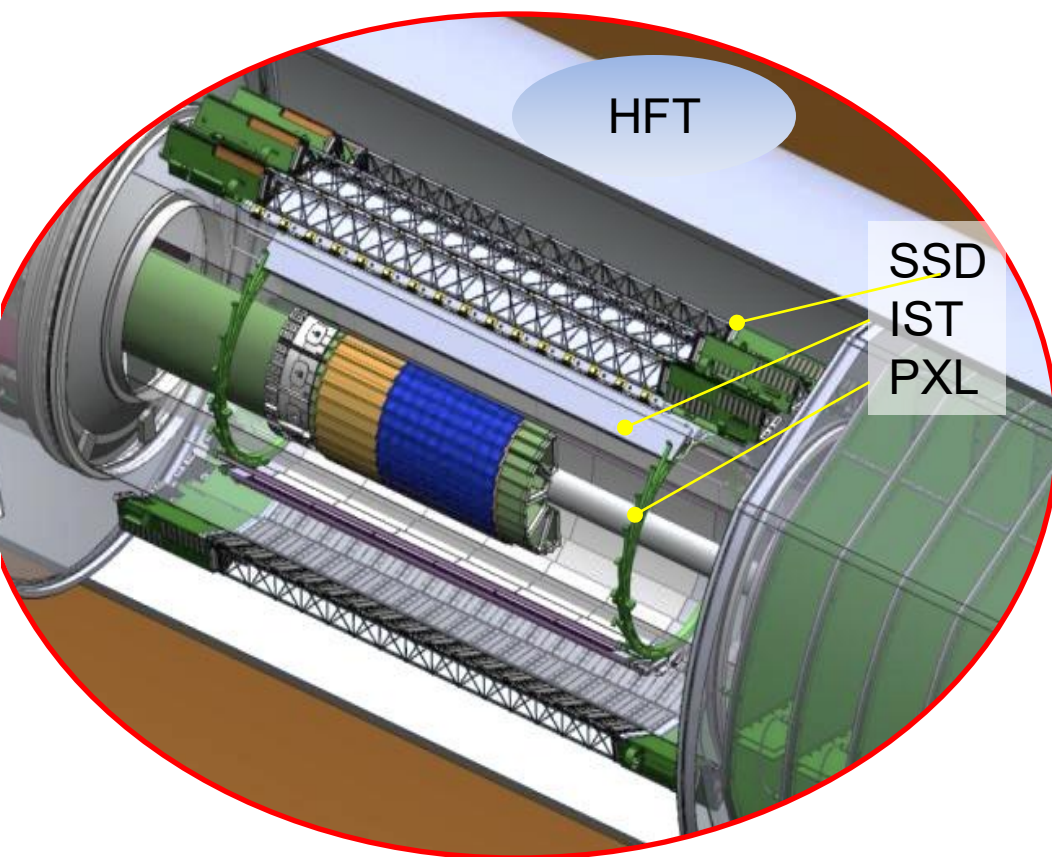


Figure 2.8 A schematic view of the Silicon detectors that surround the beam pipe.

Heavy Flavor Tracker (HFT)



| Detector | Radius (cm) | Hit Resolution $R/\phi - Z$ ($\mu\text{m} - \mu\text{m}$) | Radiation length |
|----------|-------------|---|------------------|
| SSD | 22 | 20 / 740 | 1% X_0 |
| IST | 14 | 170 / 1800 | <1.5 % X_0 |
| PIXEL | 8 | 12/ 12 | ~0.4 % X_0 |
| | 2.5 | 12 / 12 | ~0.4% X_0 |

PIXEL

- two layers
- 18.4x18.4 μm pixel pitch
- 10 sectors, delivering ultimate Pointing resolution that allows for direct topological identification of charm.
- Monolithic active pixel sensors (MAPS) technology

SSD

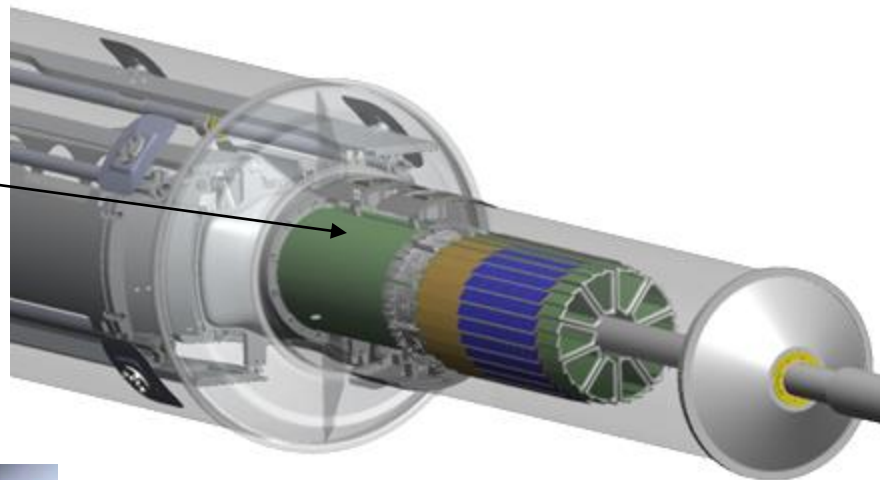
- Existing single layer detector, double side strips (electronic upgrade)

IST One layer of silicon strips along the beam direction ($r-\phi$) , guiding tracks from the SSD to PIXEL detector.

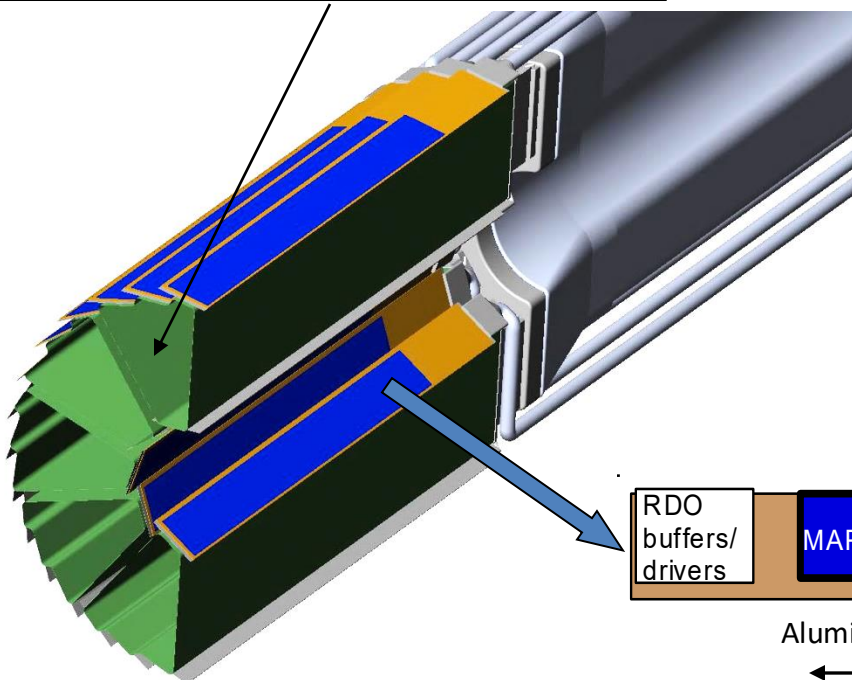
PXL Detector Mechanical Design

Mechanical support with kinematic mounts (insertion side)

carbon fibre sector tubes ($\sim 200\mu\text{m}$ thick)



Insertion from one side
2 layers
5 sectors / half (10 sectors total)
4 ladders / sector



Ladder with 10 MAPS sensors ($\sim 2 \times 2$ cm each)

RDO
buffers/
drivers

MAPS

Aluminum conductor Ladder Flat Cable

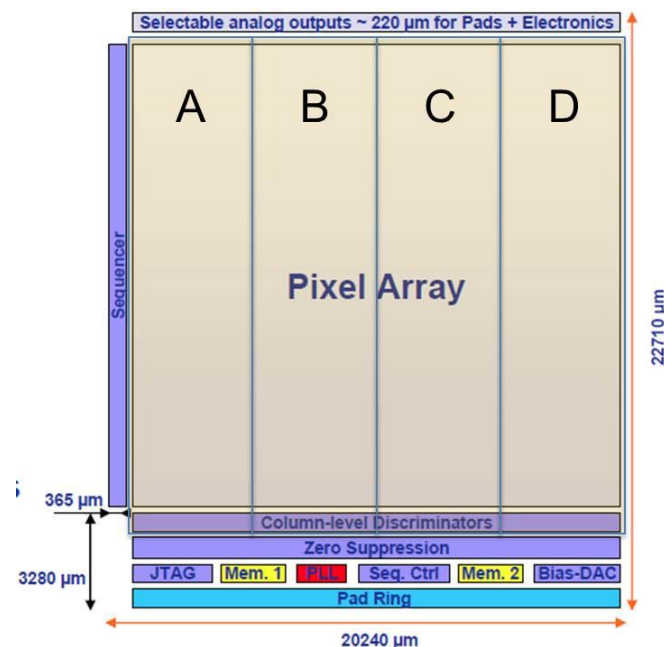
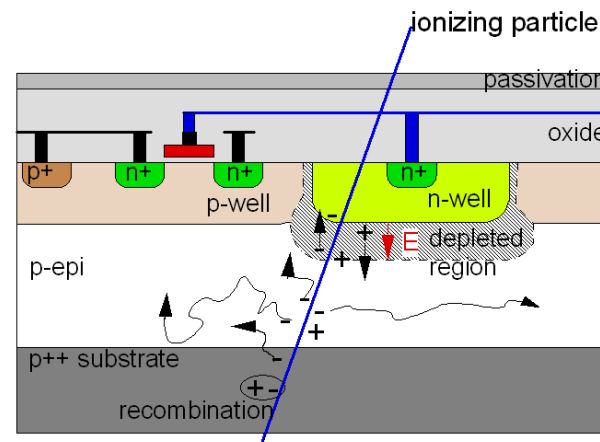
20 cm

PXL Sensor

Monolithic Active Pixel Sensor technology

Ultimate-2: third generation sensor developed for the PXL detector by the PICSEL group of IPHC, Strasbourg

- High resistivity p-epi layer
 - Reduced charge collection time
 - Improved radiation hardness
 - 20 to 90 kRad / year - $2 \cdot 10^{11}$ to 10^{12} 1MeV n eq/cm²
- S/N ~ 30
- MIP Signal ~ 1000 e⁻
- 928 rows * 960 columns = ~1M pixel
- Rolling-shutter readout
 - connects row by row to end-of-column discriminators
 - 185.6 μs integration time
 - ~170 mW/cm² power dissipation
- Configurable via JTAG
- 2 LVDS data outputs @ 160 MHz



PXL Hit Position Resolution

- *Ultimate-2* sensor geometry
 - pixel size: $20.7\ \mu\text{m} \times 20.7\ \mu\text{m}$ $\sim 6\ \mu\text{m}$ geometrical resolution
 - 3-pixel av. cluster size $\sim 3.7\ \mu\text{m}$ resolution on center-of-mass
- Position stability
 - Vibration at air cooling full flow: $\sim 5\ \mu\text{m}$ RMS
 - *Stable displacement at full air flow*: $\sim 30\ \mu\text{m}$
 - *Stable displacement at power on*: $\sim 5\ \mu\text{m}$
- **Global hit resolution:** $\Delta x \sim 6.2\ \mu\text{m}$

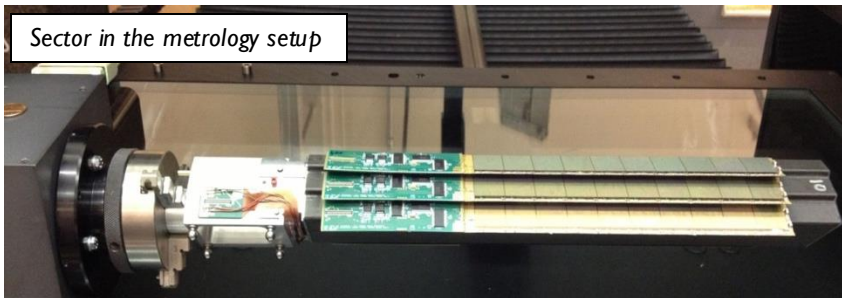
$$\Delta x \sim 6.2\ \mu\text{m}$$

$$r_1 = 2.8\ \text{cm}$$

$$r_2 = 8\ \text{cm}$$

$$\Delta v = \Delta x \bullet \sqrt{\frac{r_2^2 + r_1^2}{(r_2 - r_1)^2}}$$

HFT DCA pointing resolution:
 $(10 \oplus 24/p)\ \mu\text{m}$

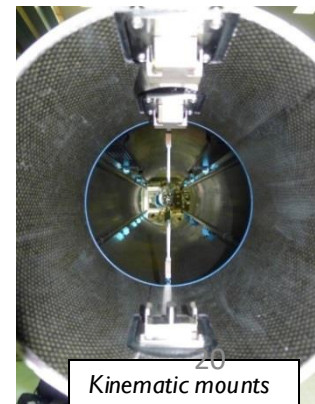


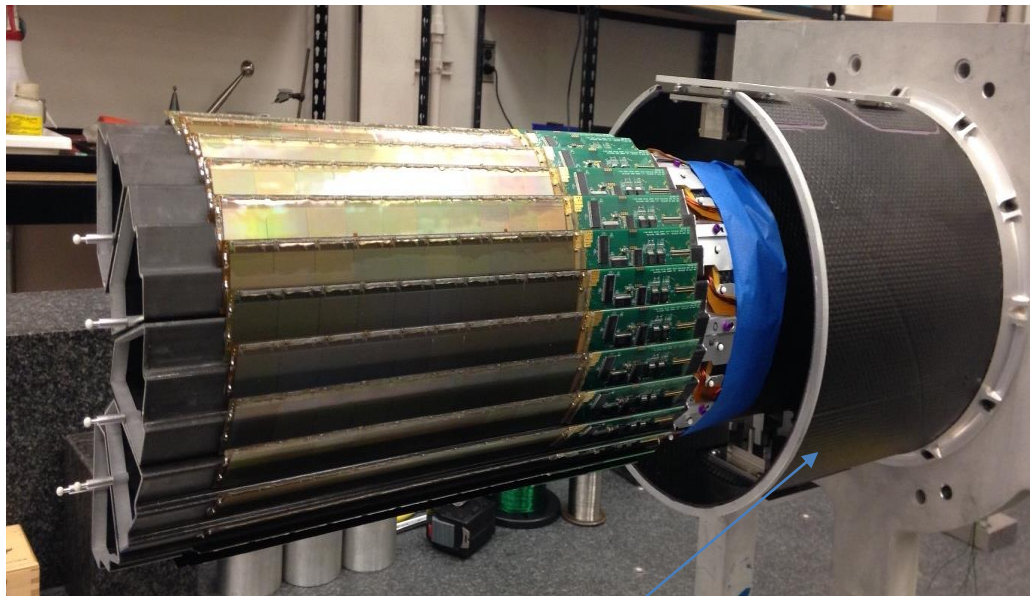
► Metrology survey

- 3D pixel positions fully mapped and related to kinematic mounts

► Novel insertion approach

- Inserted along rails and locked into a kinematic mount inside the support structure
- Capability to fully replace PXL within 12 hour





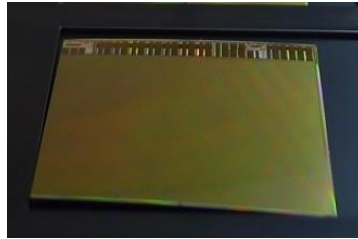
duplicate, truncated PXL
support tube with kinematic
mounts

- After assembling sectors in a half shell sector tooling balls measured with touch probe relative to kinematic mount coordinate frame
- Since the shells are supported the same way in the CMM and in the STAR installation the relative pixel position mapping is not disturbed

PXL Material Budget

- Thinned Sensor

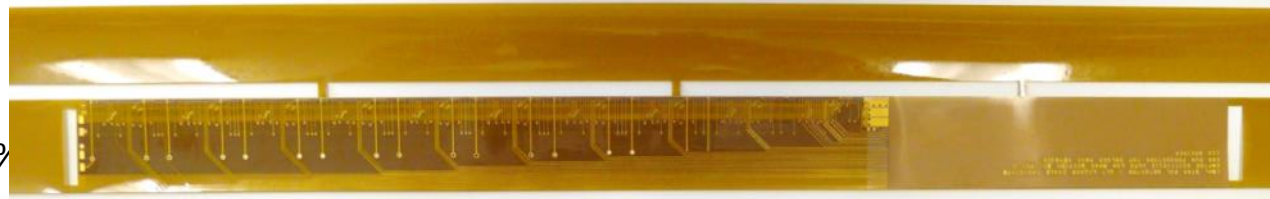
- 50 μm
- 0.068% X_0



- Curved sensor
- 40-60% yield after thinning, dicing and probe testing

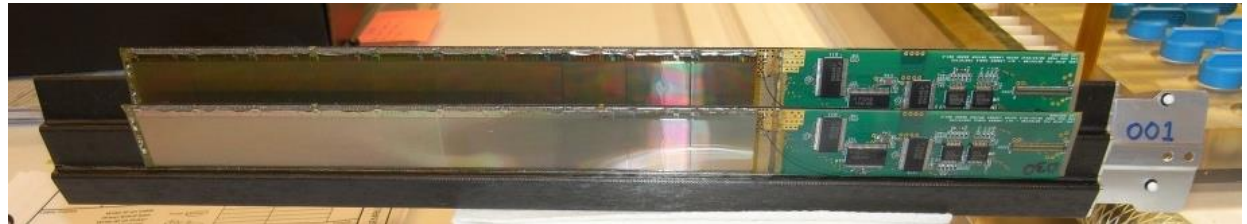
- Flex Cable

- Aluminum-Kapton
- two 32 μm -thick Al layers
- 0.128% X_0
 - Copper version \rightarrow 0.232%



- Carbon fiber supports

- 125 μm stiffener
- 250 μm sector tube
- 0.193% X_0



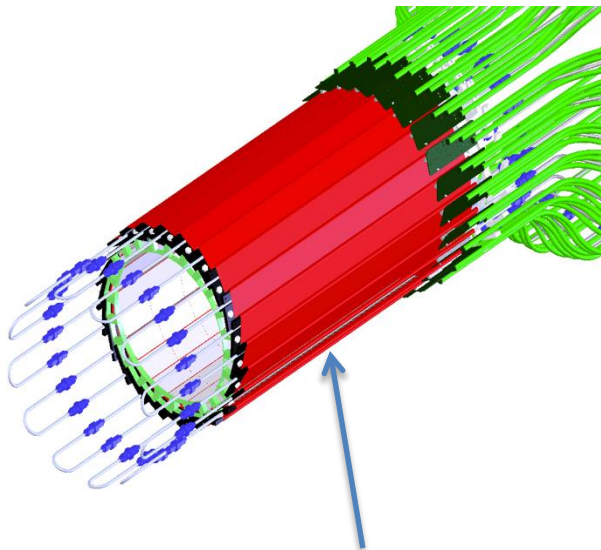
- Cooling

- Air cooling: negligible contribution

- **Total material budget on inner layer: 0.388% X_0**
(0.492% X_0 for the Cu conductor version)

HFT DCA pointing resolution:
(10 \oplus 24/p) μm

Intermediate Si Tracker



24 ladders, liquid cooling



Details of wire bonding

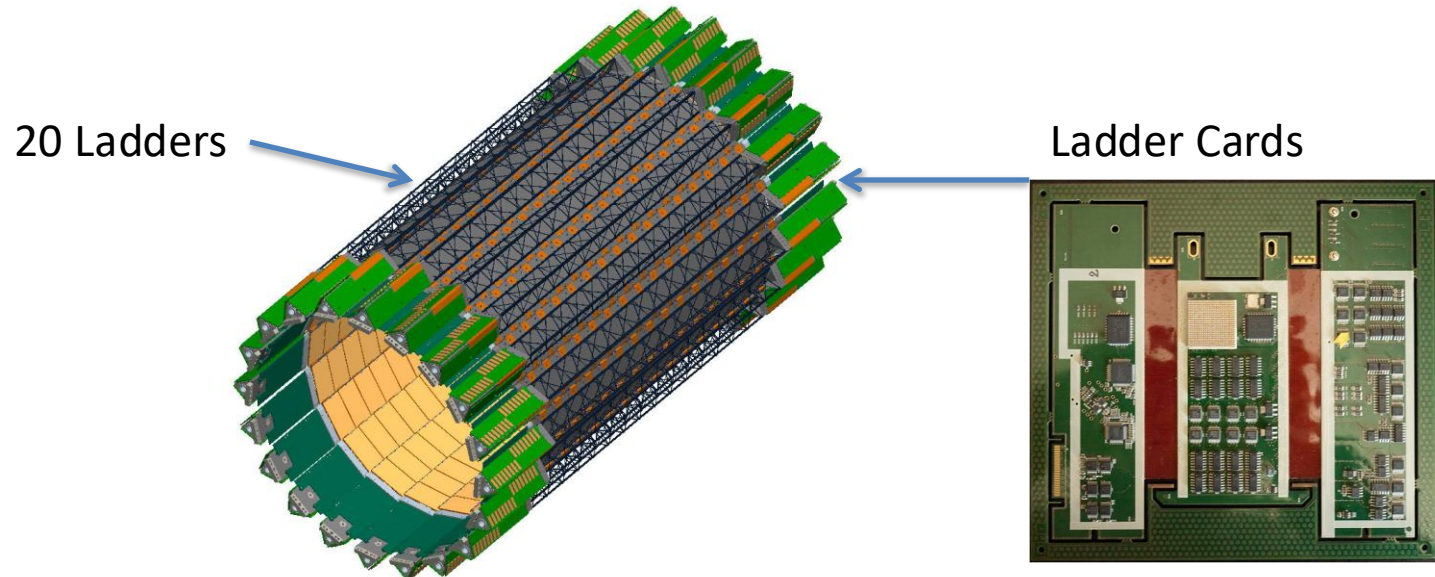
Prototype Ladder

$S:N > 20:1$

$>99.9\%$ live and functioning channels



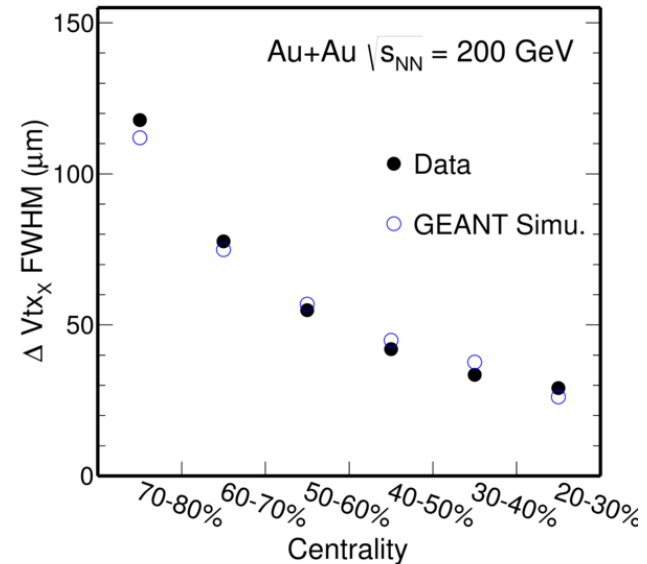
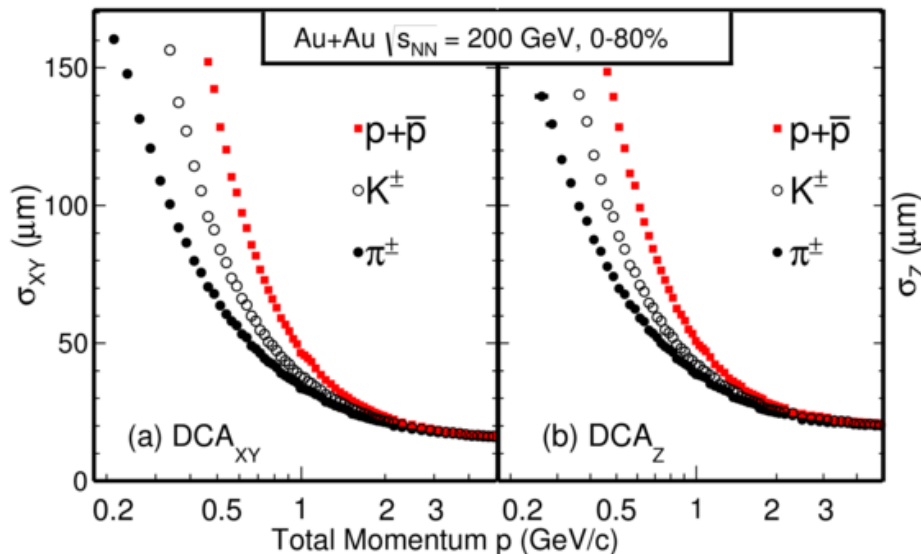
Silicon Strip Detector (SSD)



- The ladders and Si-sensors was from existing detector
- Upgrade readout system with new ladder cards on detector, RDO cards, and cooling system

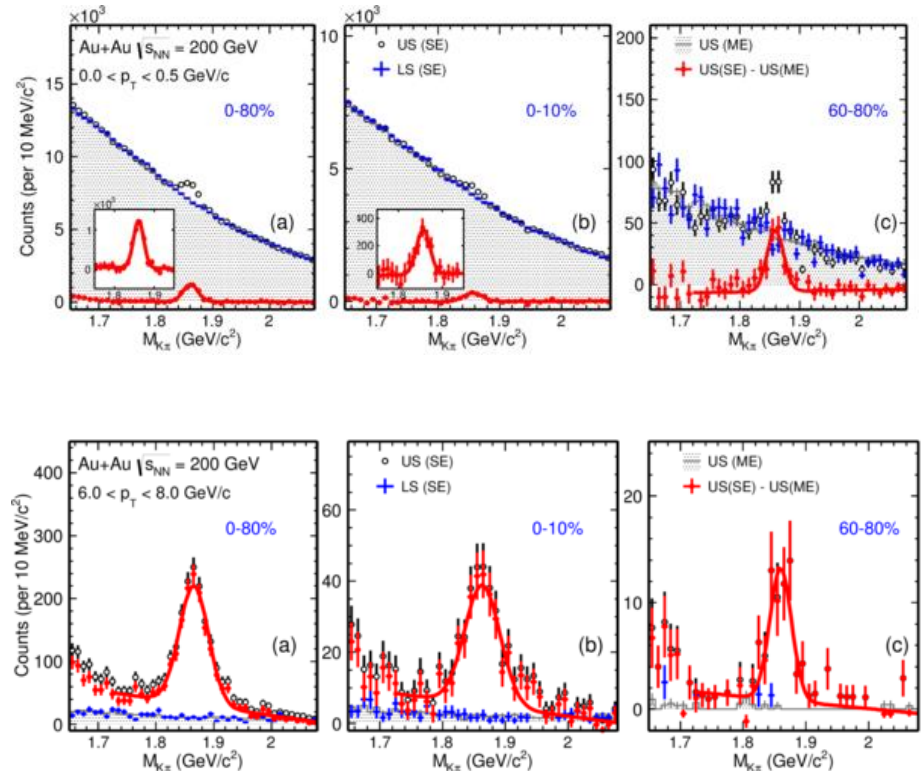
HFT performance

- Pointing resolution was determined in Au+Au collisions at 200 GeV in transverse plane and longitudinal. Measurements are in agreement with expectations.
- Important also to take into account the vertex resolution vs. centrality, particular for the most peripheral collisions



D⁰ spectra

- We have achieved very good significance for D⁰
- Low p_T is difficult due to the pileup and miss matched hit points



Physics of the Heavy Flavor Tracker at STAR

- Direct HF hadron measurements (p+p and Au+Au)
 - (1) Heavy-quark cross sections: $D^{0\pm*}$, D_S , Λ_C , B , ...
 - (2) Both spectra (R_{AA} , R_{CP}) and v_2 in a wide p_T region: 0.5 - 10 GeV/c
 - (3) Charm hadron correlation functions, heavy flavor jets
 - (4) Full spectrum of the heavy quark hadron decay electrons
- Physics
 - (1) Measure heavy-quark hadron v_2 , heavy-quark collectivity, to study the medium properties e.g. light-quark thermalization
 - (2) Measure heavy-quark energy loss to study pQCD in hot/dense medium e.g. energy loss mechanism
 - (3) Analyze hadro-chemistry including heavy flavors

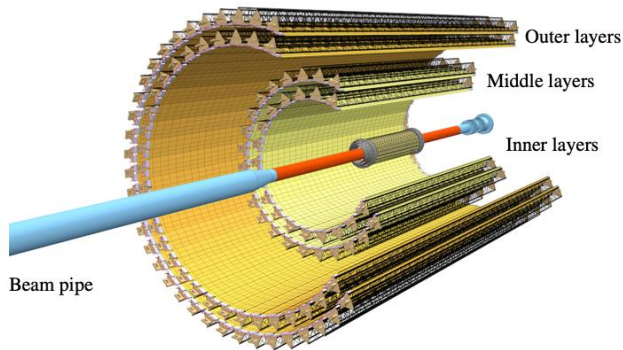
Timeline

- R&D 2003- LBL with IHPC, Strasbourg for MAPS sensors
- 2008 Project start ; 2010-2014 construction
- 2013 Commissioning run
- 2014-16 Physics
 - 14: AuAu
 - 15: pp
 - 16: AuAu dAu
- 2017 Removed from STAR and in storage
- 2014-2023 Physics analysis and papers

Next Generation MAPS

- For the upgrade of the ALICE detector in the current RUN-3 at LHC, the collaboration developed a next generation MAPS sensors
 - Faster readout time (~ 5 micro sec)
 - Better radiation hardness
 - Pixels size 30×30 micron

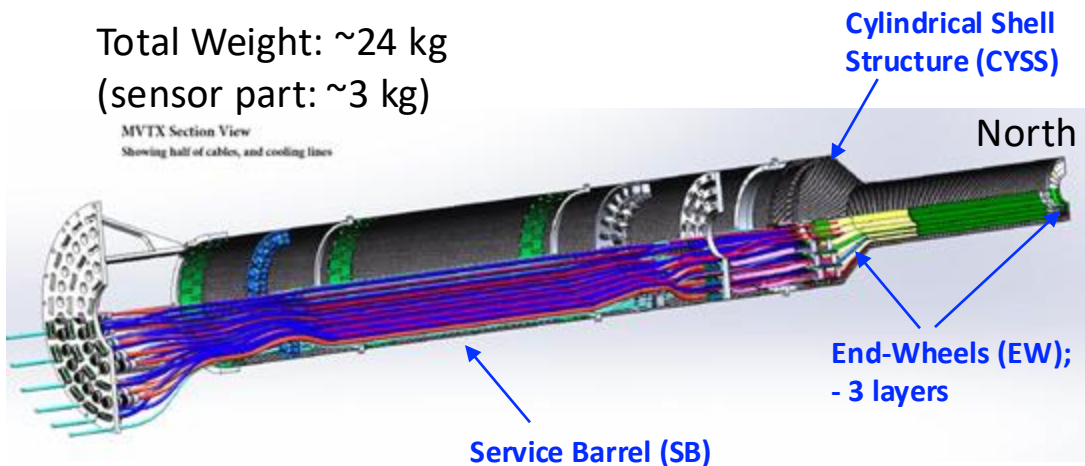
See e.g. <https://arxiv.org/pdf/2111.08301.pdf>



MVTX - sPHENIX Inner Most Detector for HF physics

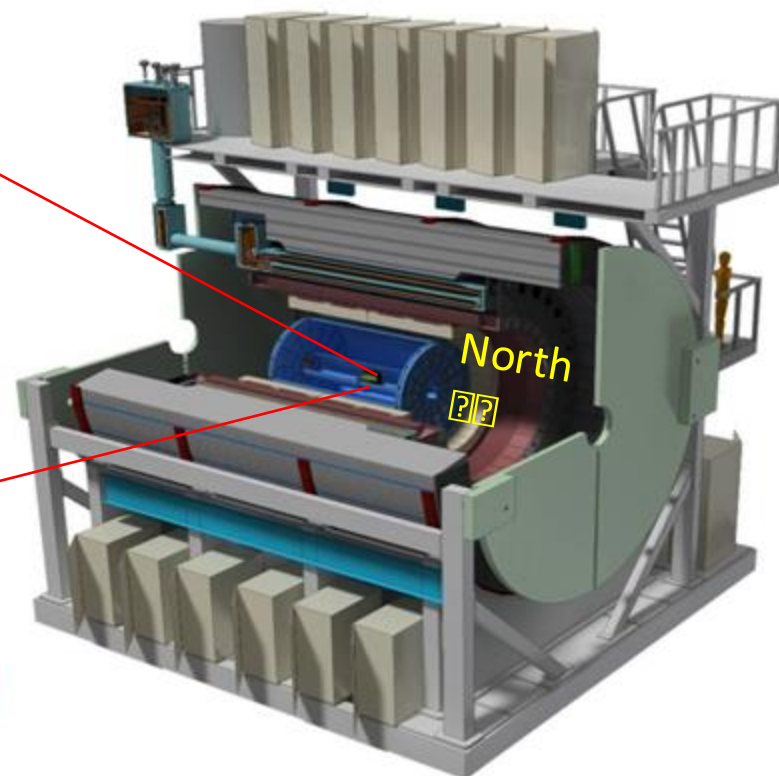
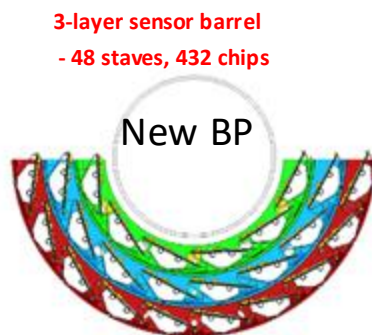
Carb. Fib. Comp./CFC = EW, CYSS, SB

Total Weight: ~24 kg
(sensor part: ~3 kg)



MVTX parameters: L = 271 mm

| R (mm) | min | mid | max |
|---------|-------|-------|-------|
| Layer 0 | 24.61 | 25.23 | 27.93 |
| Layer 1 | 31.98 | 33.35 | 36.25 |
| Layer 2 | 39.93 | 41.48 | 44.26 |



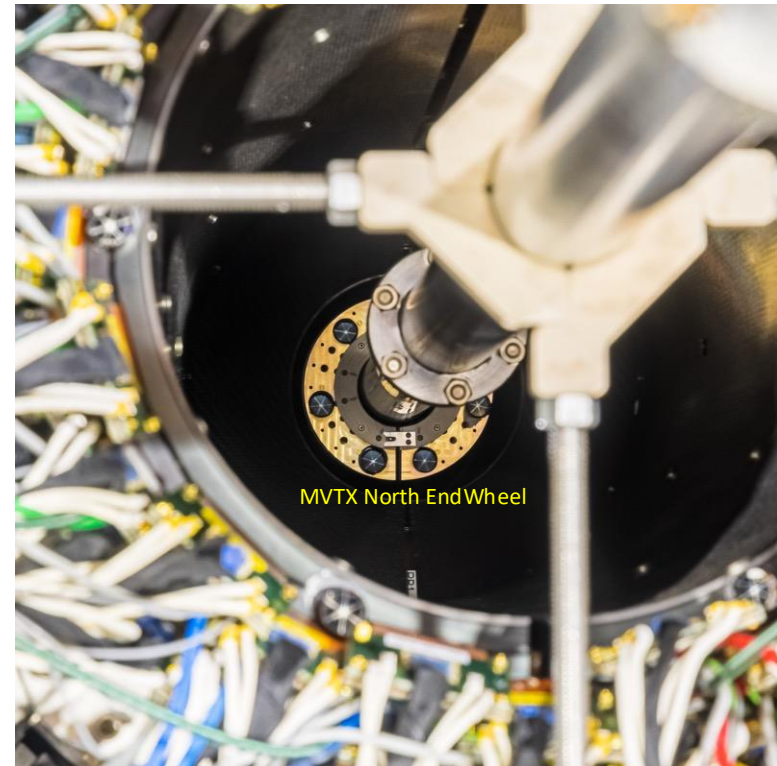
sPHENIX MVTX Photos

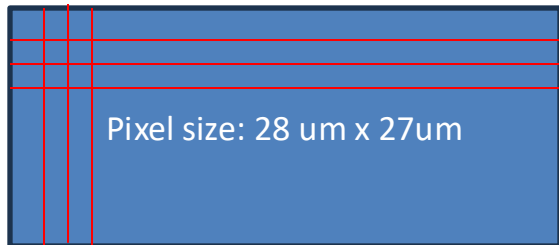
Viewed from South right before the installation: One can clearly see the service lines inside the Service Barrel (SB):

Blue: data cable, Green: Cooling air, Red/Black/White: LV power



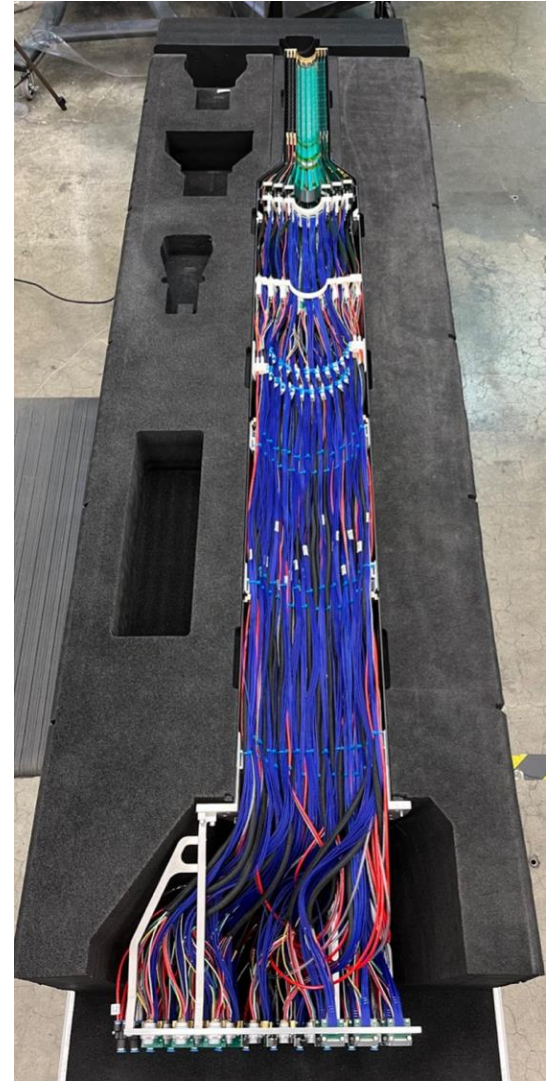
Viewed from North after installation

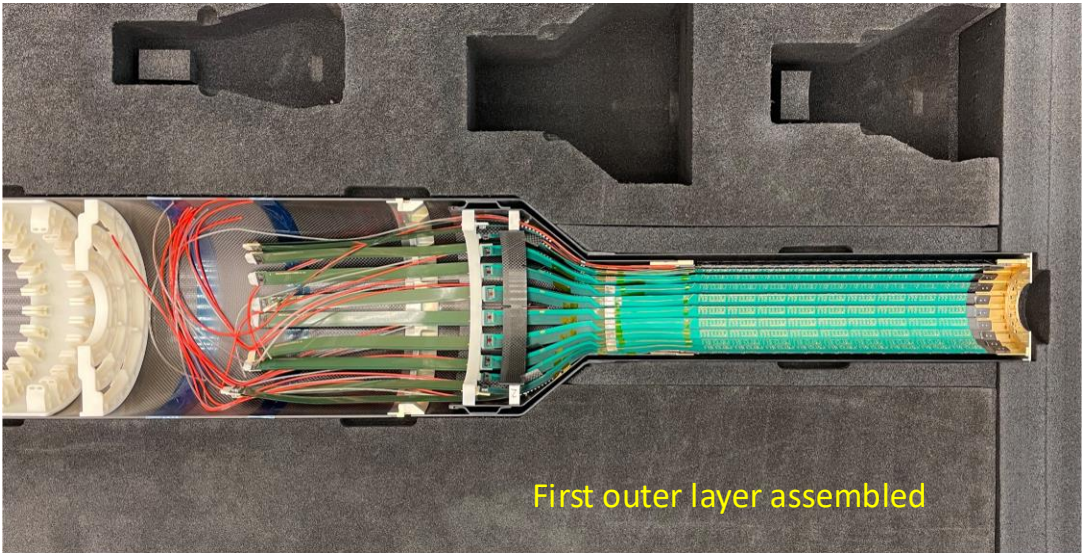




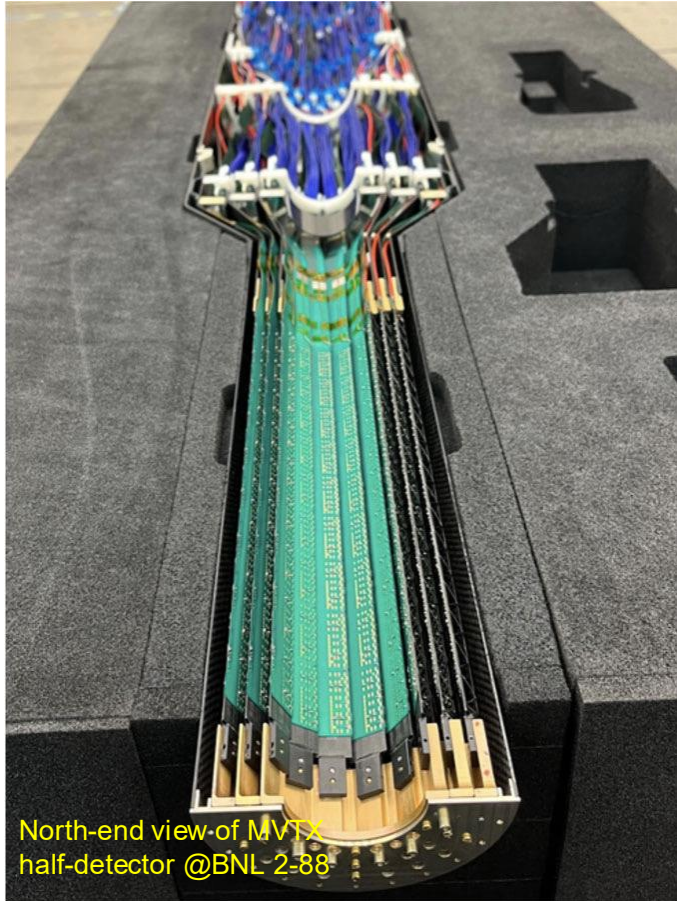
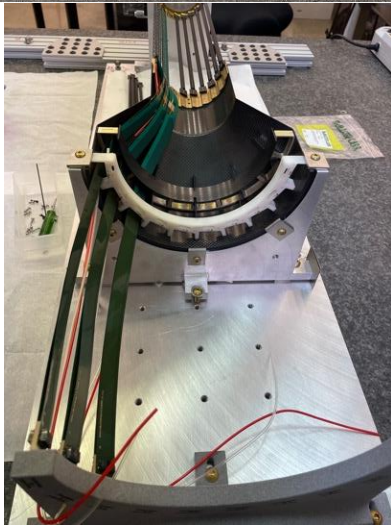
512 rows
(~1.5cm)

1024 columns (~3cm)





First outer layer assembled



North-end view of MVTx
half-detector @BNL 2-88

- MAPS detector has matured a lot, and next generations will be used at eRHIC in EPIC detector and at another upgrade to ALICE
- TPC are used at collider experiments and also in neutrino physics experiments
- More questions?

ideas to explore

- What are the applications for MAPS in current and planned experiments?
- Radiation damage is important to understand at RHIC, LHC, and space. How are this being investigated?
- Where does radiation have a positive impact?
- Where has Nuclear Physics impacted society with inventions and applications?

Info on PXL detector mechanics and construction

- NIM Article
 - arXiv 1710.02176
 - NIM A97(2018) 60
- Howard Wieman
 - HFT PXL mechanics
 - Forum on Tracking Detector Mechanics
 - 30 June-2 July 2014 at DESY, Hamburg
 - https://indico.cern.ch/event/287285/contributions/1640694/attachments/534386/736809/PXL_mechanics.pdf

Spatial mapping of the pixels

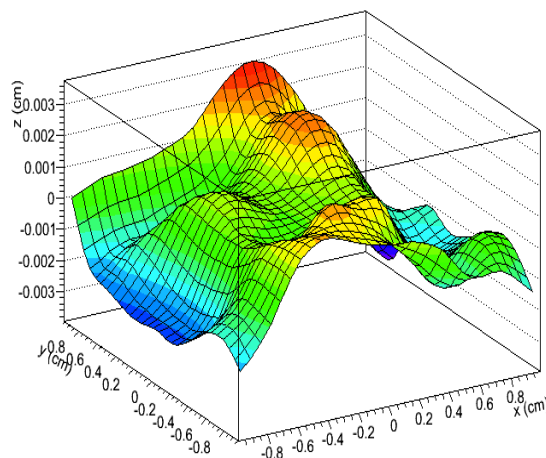
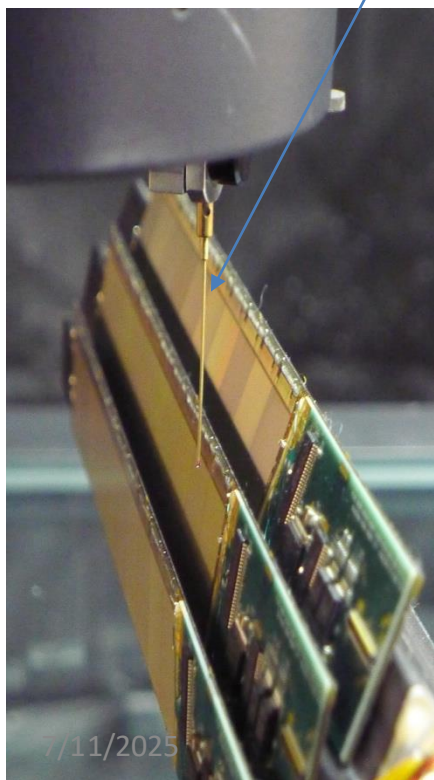
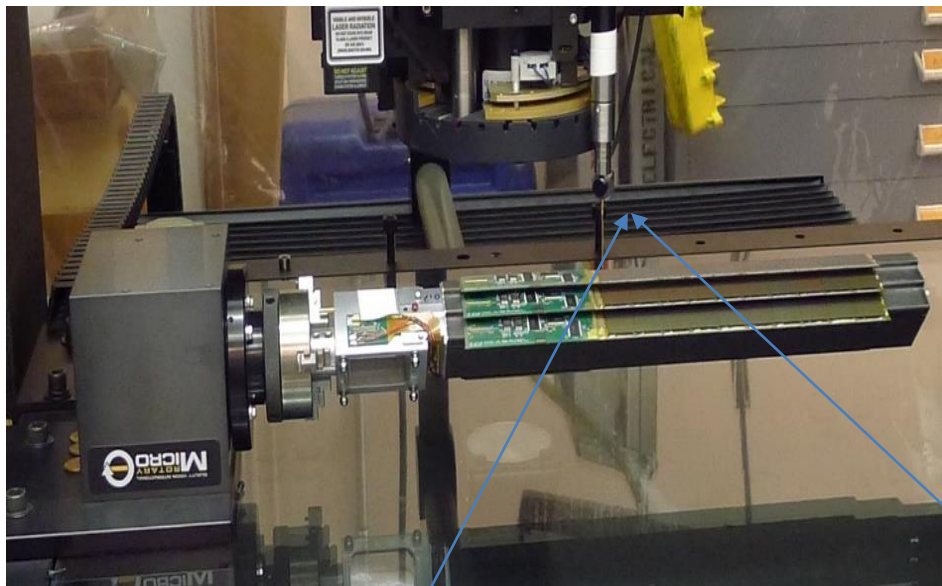
Pixel locations determined with CMM equipment to within 10 μm prior to installation in STAR

Programmed CMM Measurement method[#]:

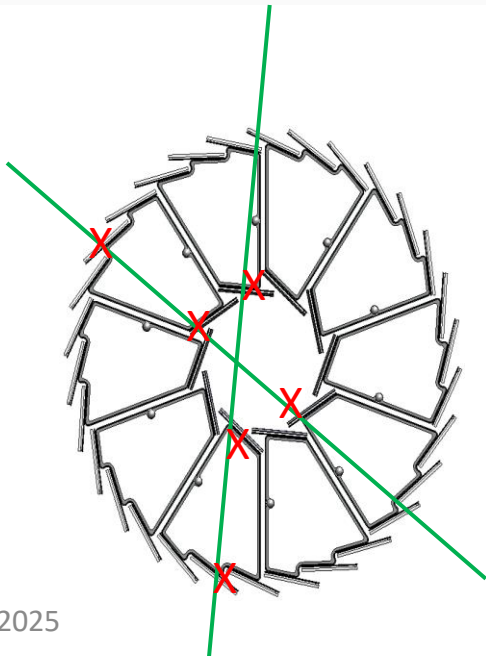
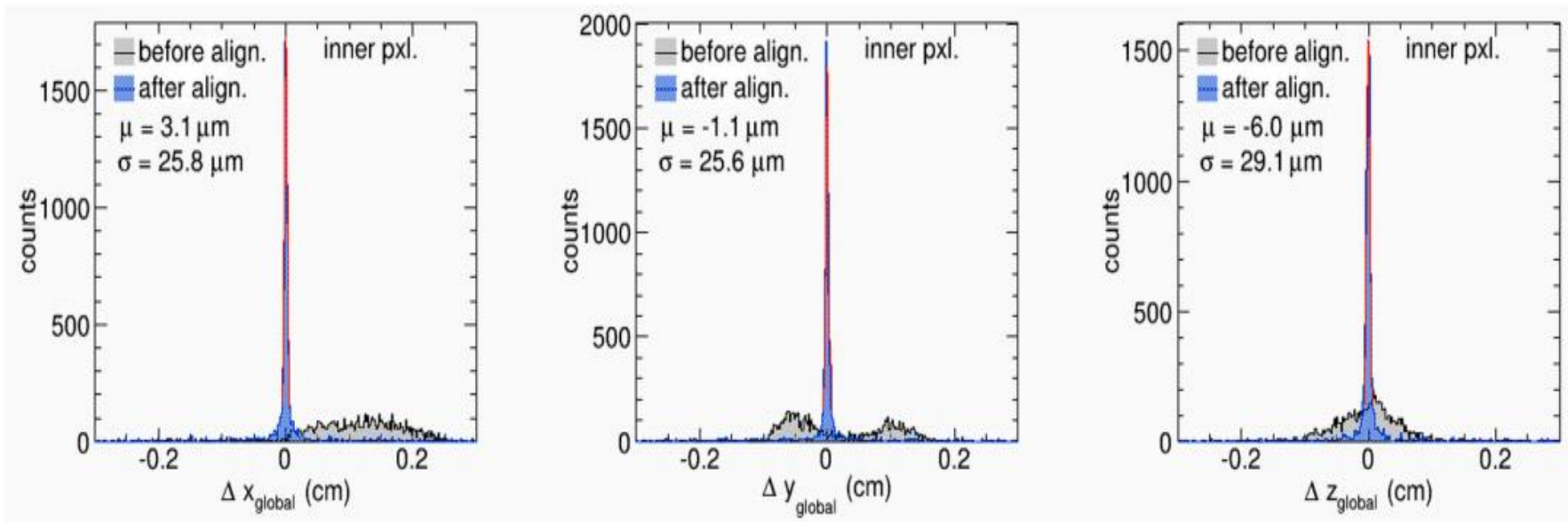
- All pixels located on a sector with respect to 3 sector tooling balls
 - 2 Lithography points on the chips measured with optical head
 - Chip surface profile measured with 11 x 11 point pattern using a Feather Probe*. Using a touch probe permits picking up over hung surfaces

PXL sensor surface profile from survey:
 $\pm 30 \mu\text{m}$ > PXL hit error,
and the chip to chip surface deviation
along the ladder surface is still larger,
but all of this is then corrected with the
spatial map
Parametrized by 5*5 spline fct

Full sector measurement takes ~ 8 hours



Final operating pointing performance in STAR



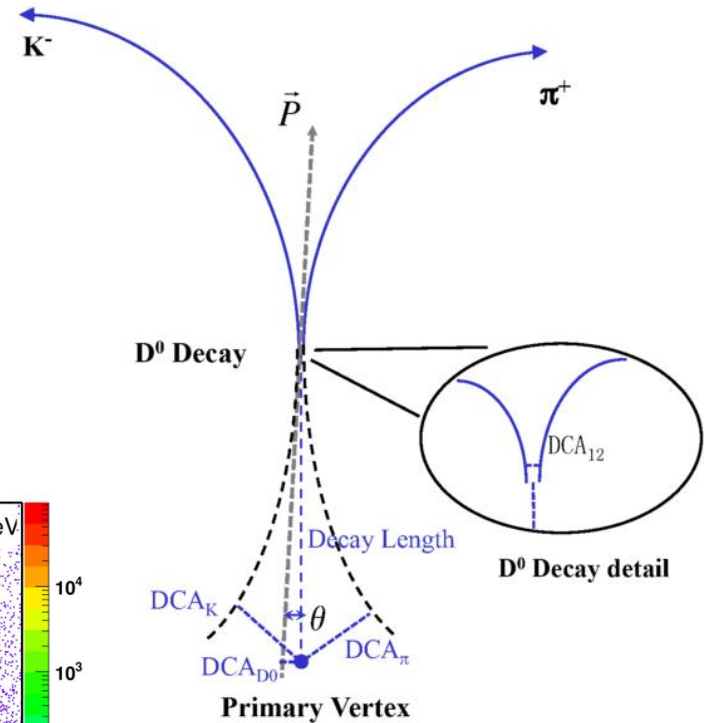
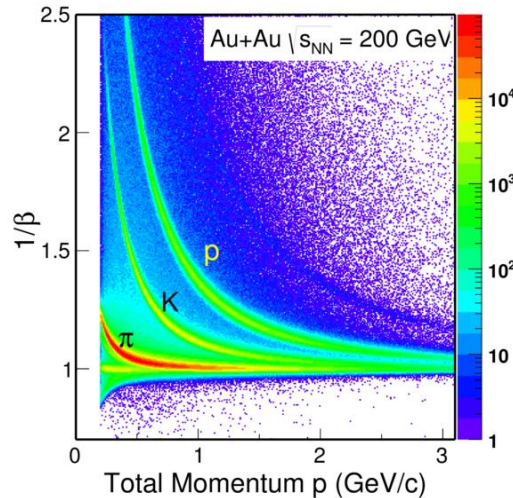
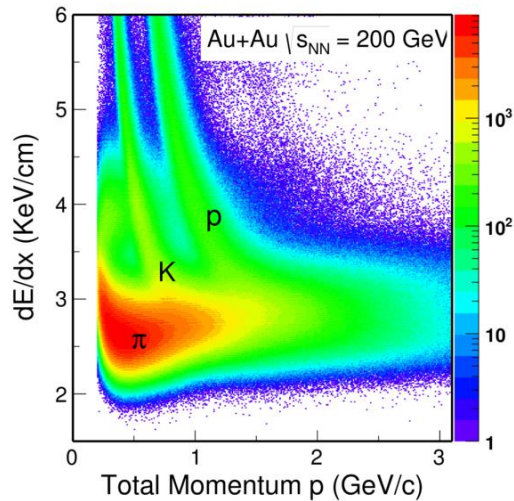
Cosmic ray result

Excellent half to half pointing, sub 30 μm
But after half to half alignment which was required to correct poor reproducibility of kinematic mount seating

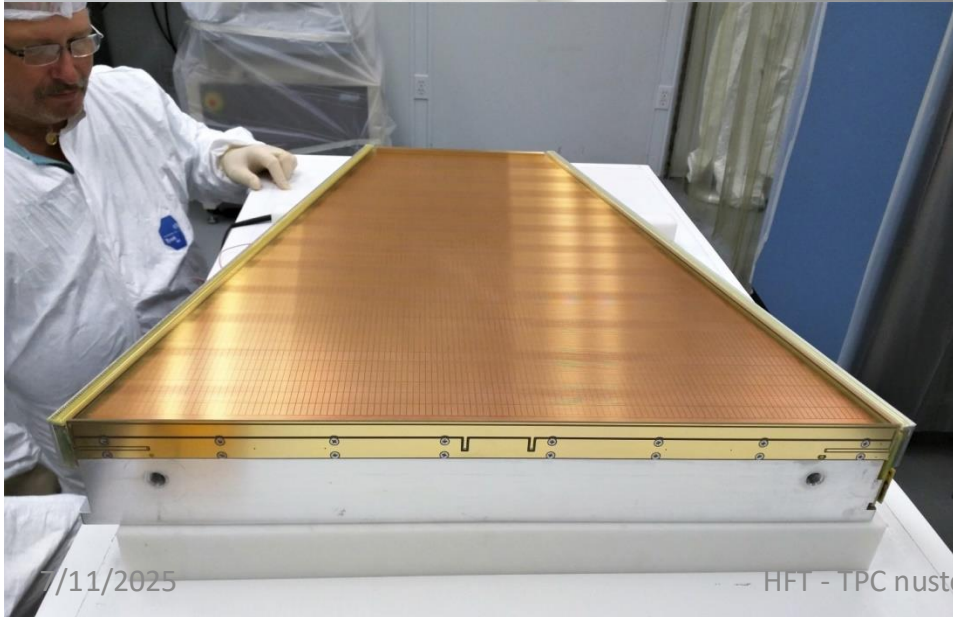
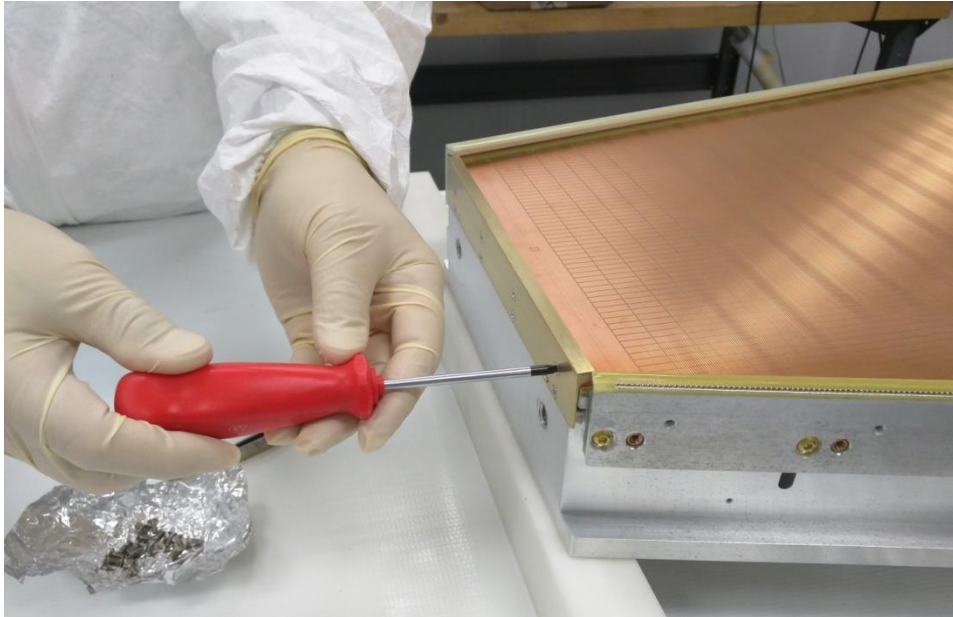
Check alignment with very low luminosity AuAu also

D^0 reconstruction

- Use topological variables
- Use particle ID



Grid Leak Walls checked

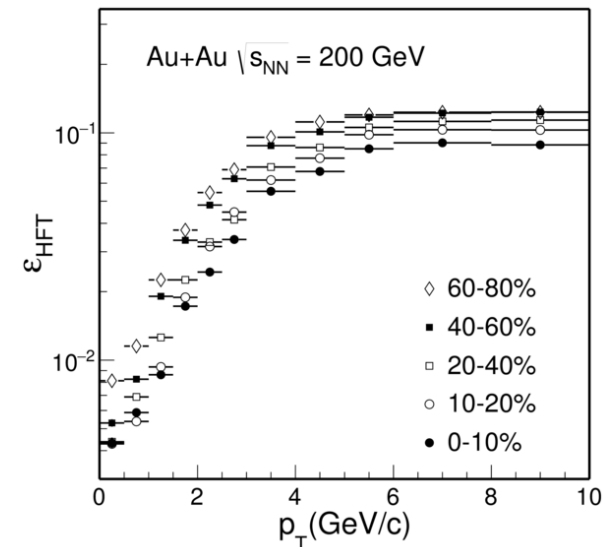
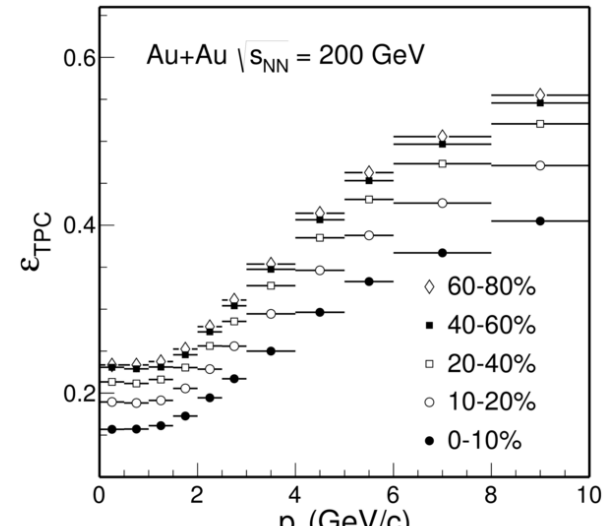


- The narrow end uses a simple brass wall to terminate the array of wires
 - Ground Potential
 - No bias required
 - Anode wires > 10 mm away
- The wide end uses a G10 PCB board to terminate the array
 - Inside wall is grounded to the strongback.
 - Anode wires > 10 mm away
 - Outside wall is used to suck ions off the Anode wires of the outer sector
 - No shield wall on outer
 - So requires ~750 volts (DC) to suck ions across the gap
 - Outer Sector Anode wires > 2 cm away
 - 3 Pads & 3 voltages (-115 V, ~750 V & ground)

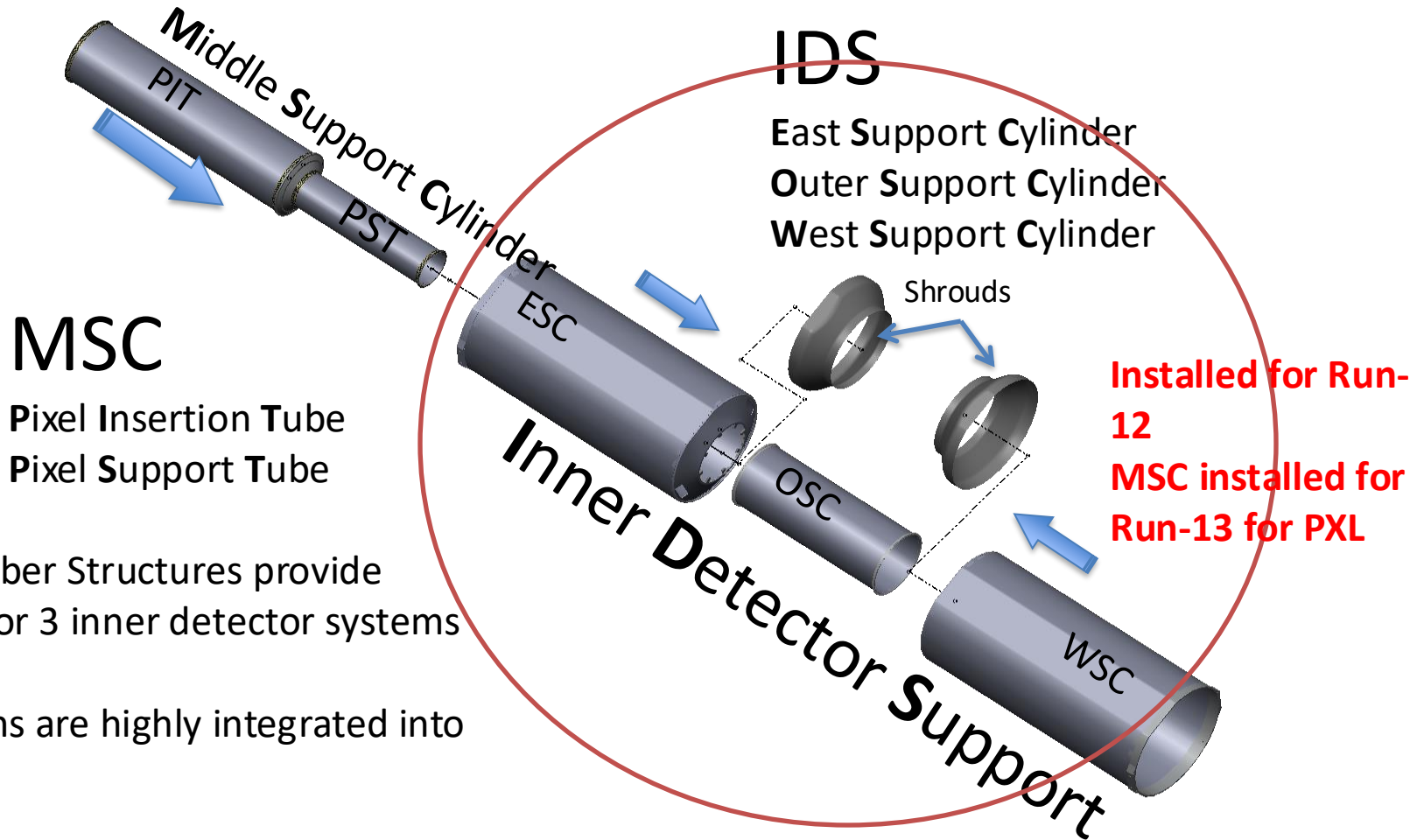
Courtesy Jim Thomas

Some words on efficiency

- We have applied two methods to evaluate efficiencies
- Fast simulation data driven to replicate multi dimensional basic observables
- Geant embedding with displaced geometries
- Methods agrees well



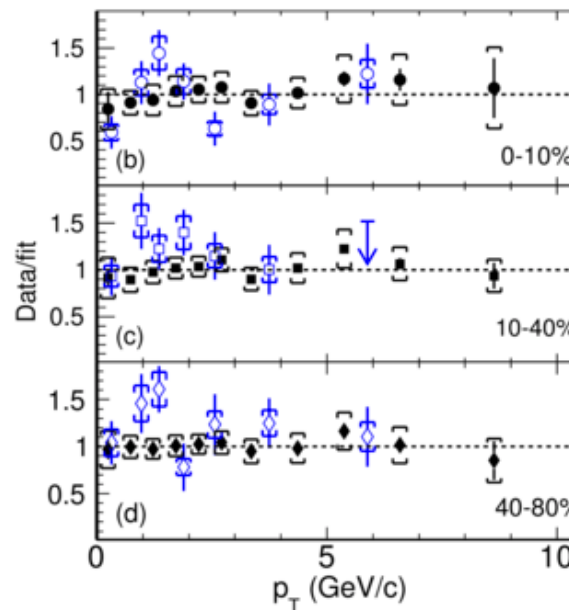
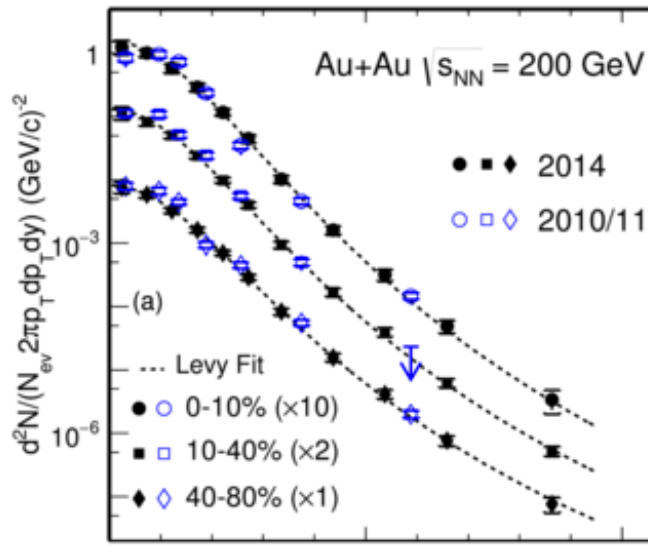
Inner Detector Support (IDS)



Carbon Fiber Structures provide support for 3 inner detector systems and FGT.
All systems are highly integrated into IDS.

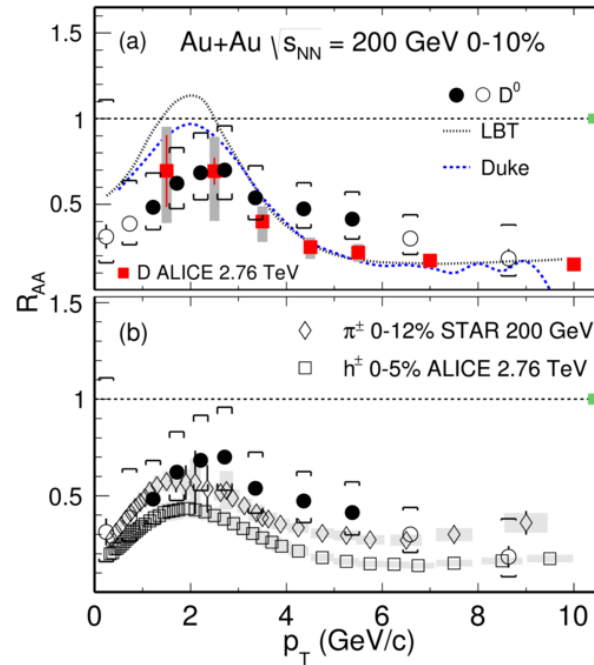
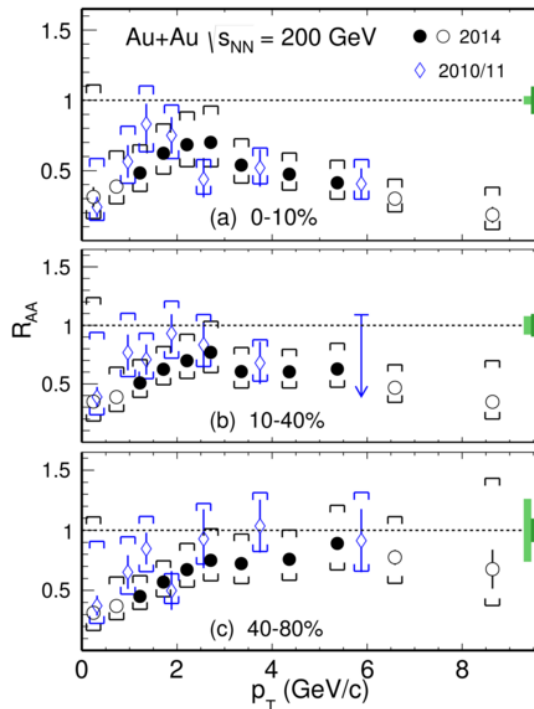
D⁰ spectra

- Precise measurements extends to low p_T and non-central collisions. Data from 2014
- Results consistent with 2010/11 TPC only analysis
- Data from submitted paper: arXiv 1812.10224



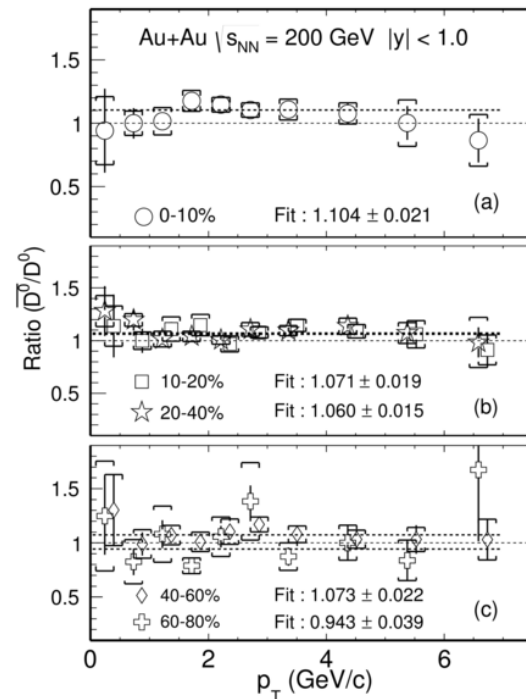
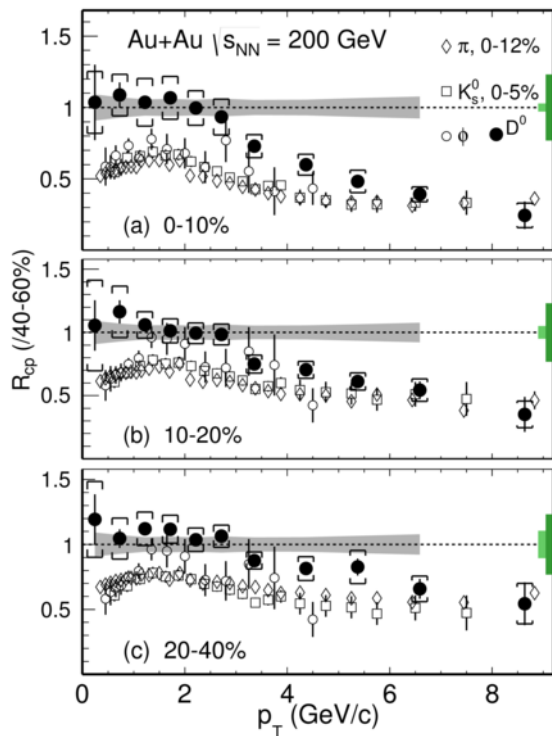
$D^0 R_{AA}$

- $R_{AA} < 1$ for 0-10% for all p_T
- Suppression at high p_T increases for more central collisions
- Same trends as at LHC and for light mesons



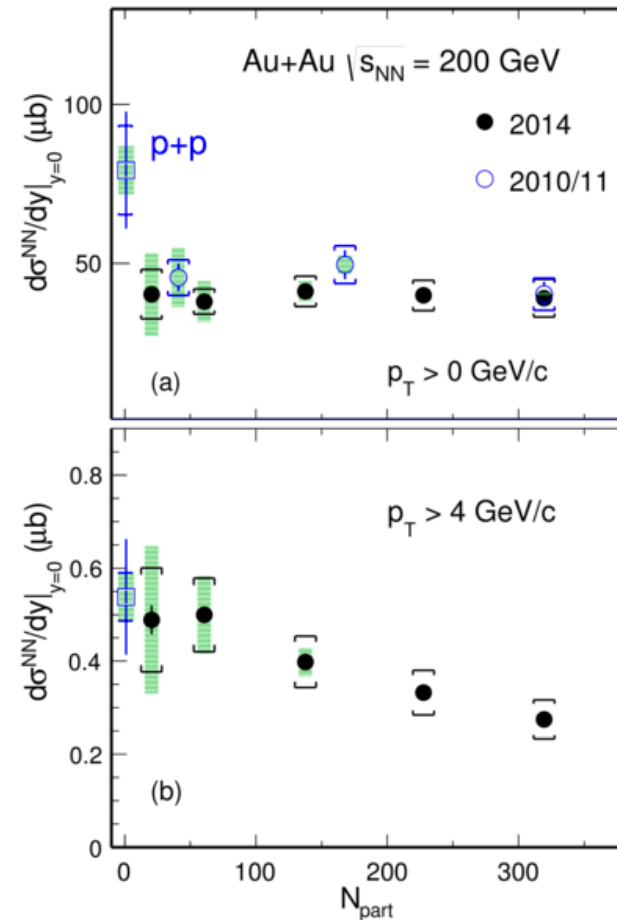
$D^0 R_{CP}$

- Significant suppression at high p_T
- Matches theoretical calculations
- $D^0\text{-bar}/D^0$ slightly greater than one
 - Possible due to slight baryon asymmetry at RHIC



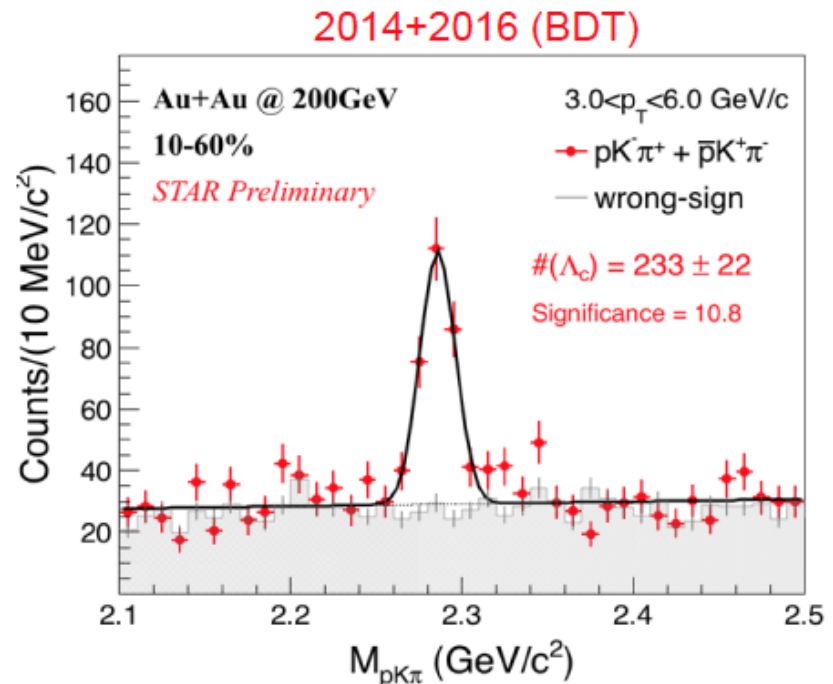
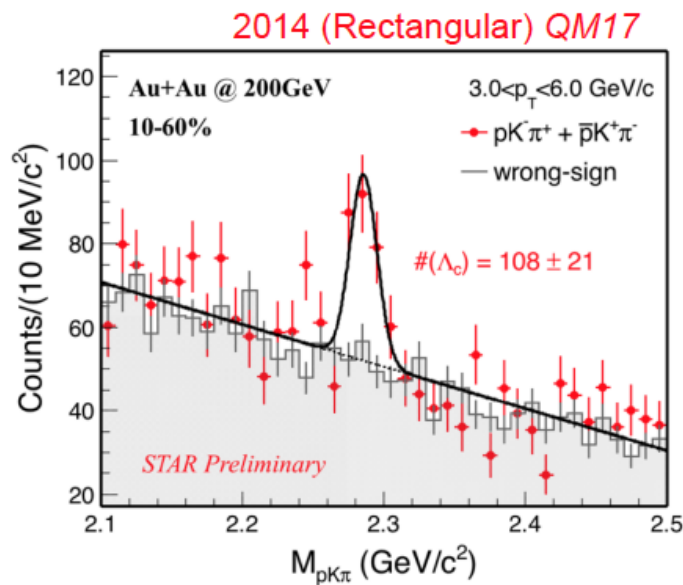
D⁰ cross section

- Total D⁰ cross section is nearly independent of centrality, and smaller than in $p+p$. For $p_T > 4$ GeV/c it decreases with centrality



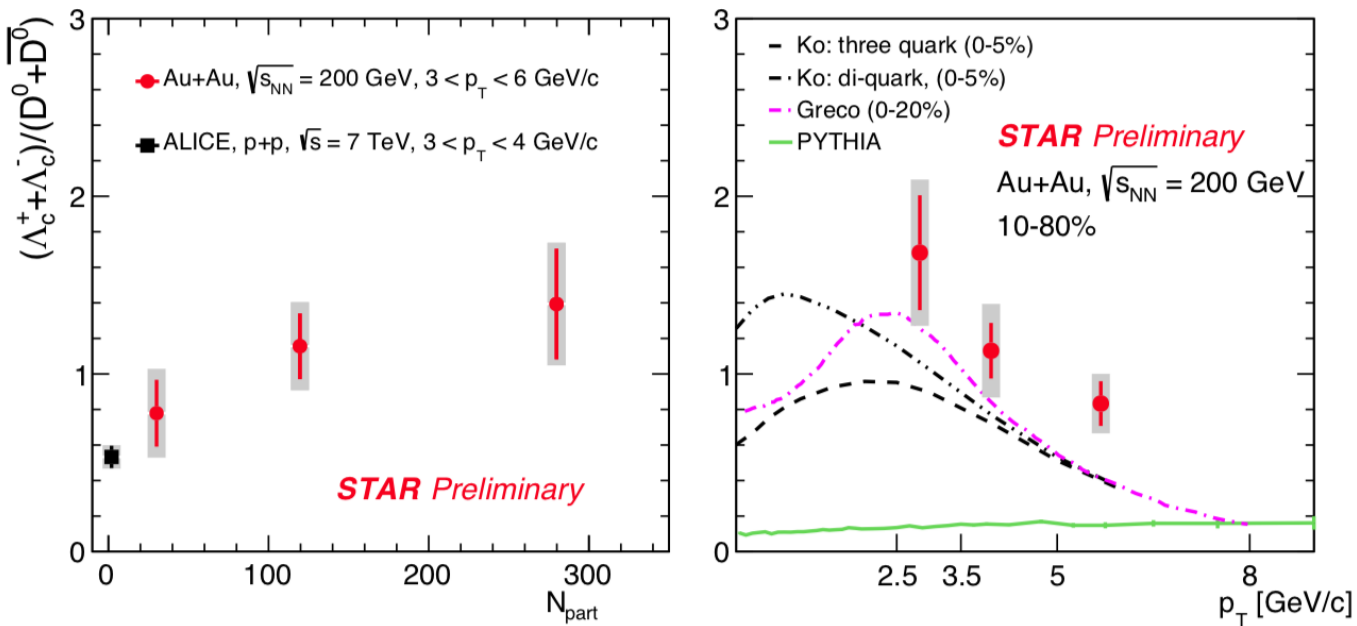
Λ_c reconstruction

- More than 50% improvement in signal significance with TMVA methods
- Includes 2016 dataset



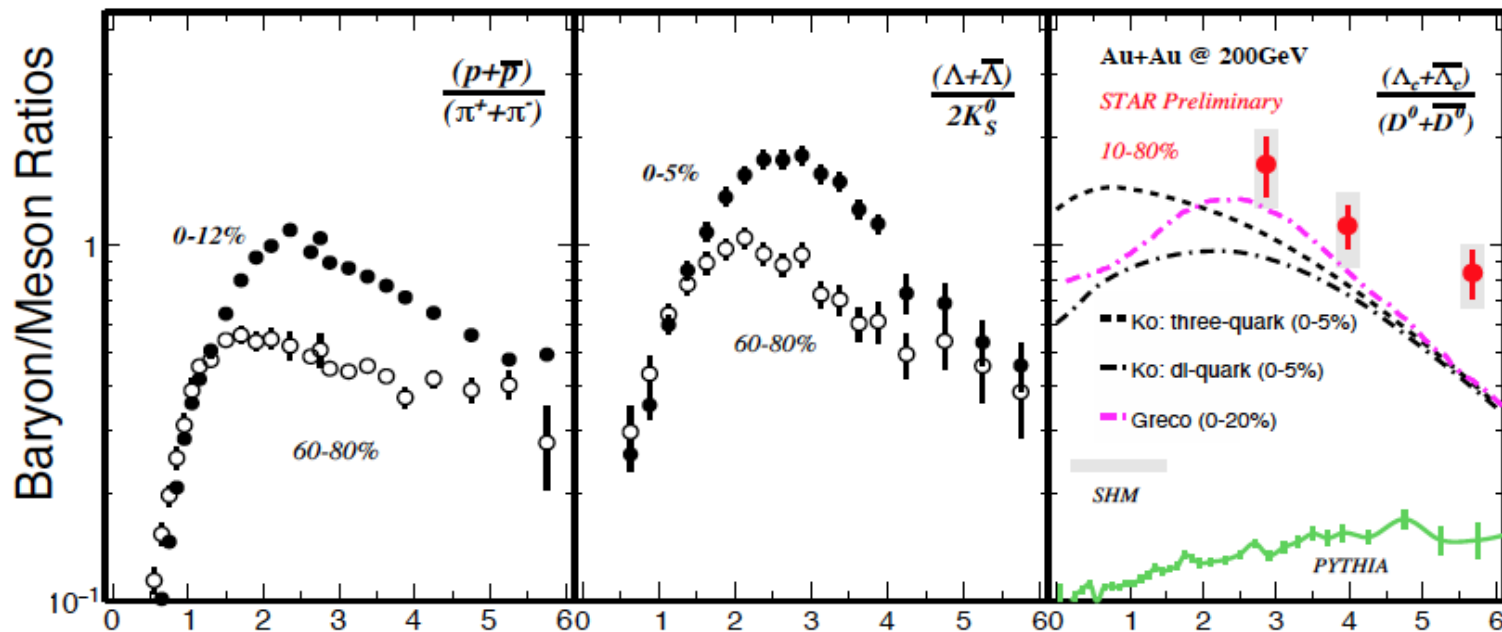
Λ_c/D^0 centrality dependence

- Λ_c enhancement increases towards more central Au+Au collisions
- Large contribution to total charm cross sections in HI



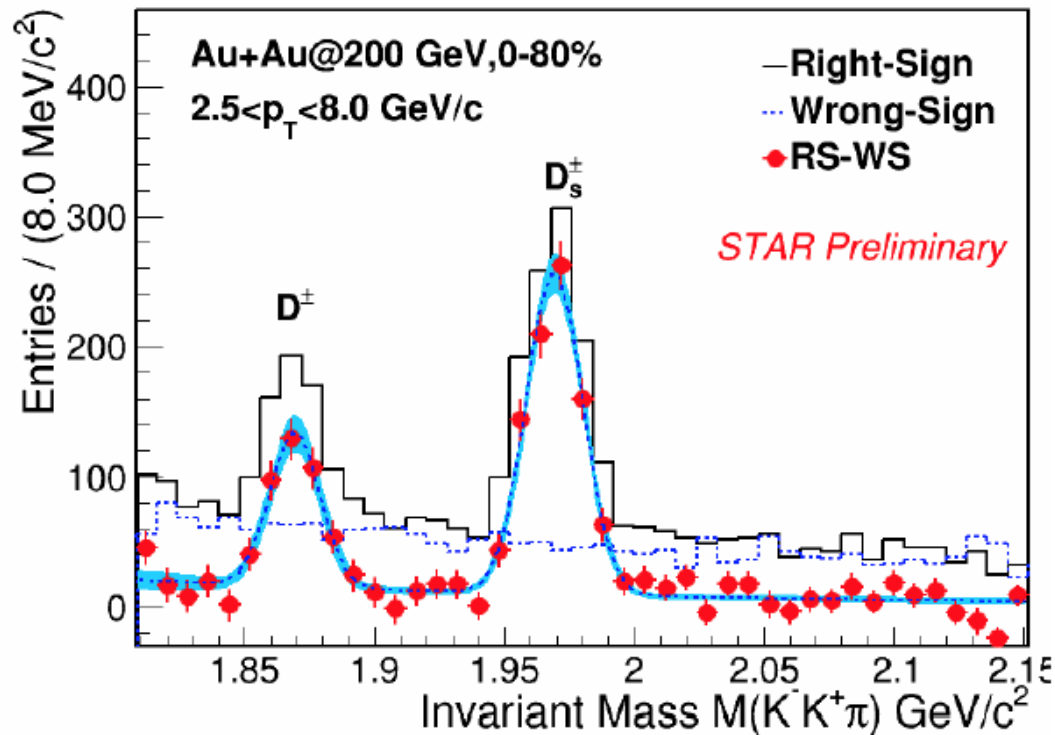
Λ_c/D^0 p_T dependence

- Significant enhancement of Λ_c/D^0 compared to p+p.
- Comparable with light flavor B-to-M ratios
- Consistent with charm quark hadronization via coalescence



Strange Charmed quarks

- Reconstruct D_s^\pm via $D_s^\pm \rightarrow \phi(1020) + \pi^\pm \rightarrow K^+K^-\pi^\pm$ decay channel
- Reconstruct D^\pm via $D^\pm \rightarrow \phi(1020) + \pi^\pm \rightarrow K^+K^-\pi^\pm$ decay channel



Total charm cross section

- D^0 yields measured down to $p_T=0$ GeV/c
- For D^{+-} , D_s Levy fits to measured spectra for extrapolation
- For Λ_c three model fits to data are used and included in systematics

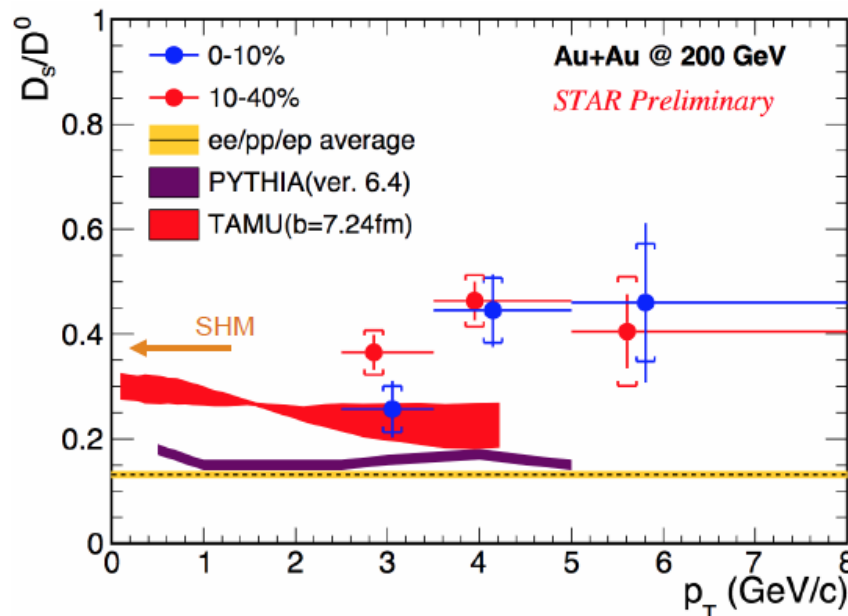
| Charm Hadron | | Cross Section $d\sigma/dy$ (μb) |
|--------------------------|---------------|--|
| AuAu 200 GeV (10-40%) | D^0 | $41 \pm 1 \pm 5$ |
| | D^+ | $18 \pm 1 \pm 3$ |
| | D_s^+ | $15 \pm 1 \pm 5$ |
| | Λ_c^+ | $78 \pm 13 \pm 28^*$ |
| | Total | $152 \pm 13 \pm 29$ |
| pp 200 GeV | Total | $130 \pm 30 \pm 26$ |

* derived using Λ_c^+ / D^0 ratio in 10-80%

Total charm cross section is consistent with p+p values
Redistributed on meson and baryons

D_s, D^0 enhancement

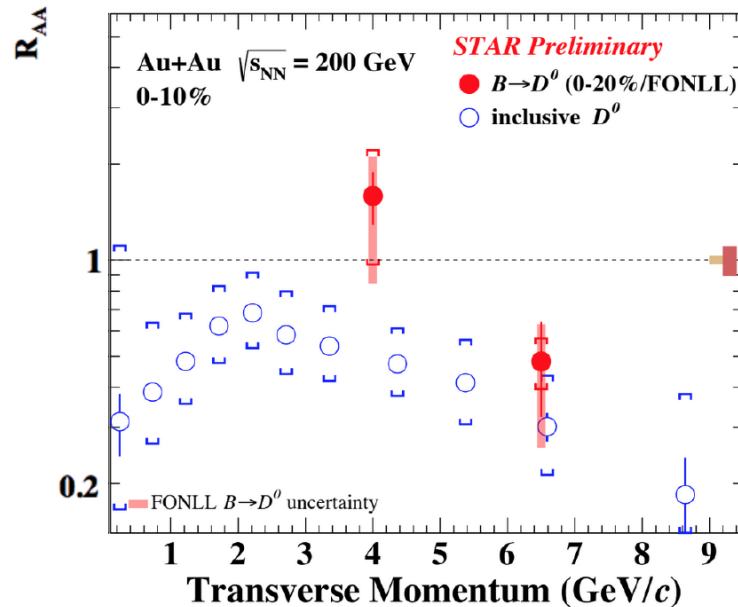
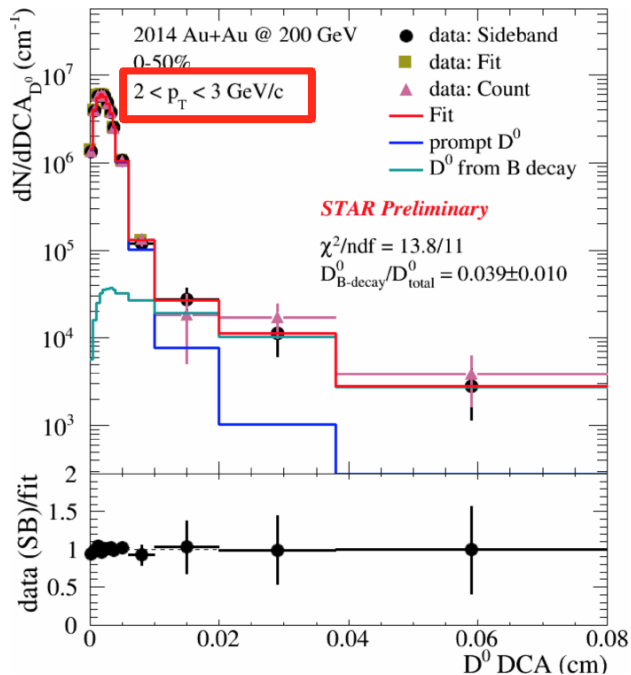
- Strong enhancement of D_s/D^0 observed in central A+A w.r.t fragmentation baseline
- ->Strangeness enhancement and coalescence
- Enhancement larger than model, particular at high p_T



ep/pp/ep avg: M Lisovsky, et. al. EPJ C 76, 397 (2016)
TAMU: H. Min et al. PRL 110, 112301 (2013)
SHM: A. Andronic et al., PLB 571 (2003) 36

Non prompt D^0 , B-decay

- Strong interaction of charm with the medium.
- What about bottom?
- R_{AA} of non-prompt D^0 extracted.
- Improved signal significance using BDT
- Will get results form combined data set

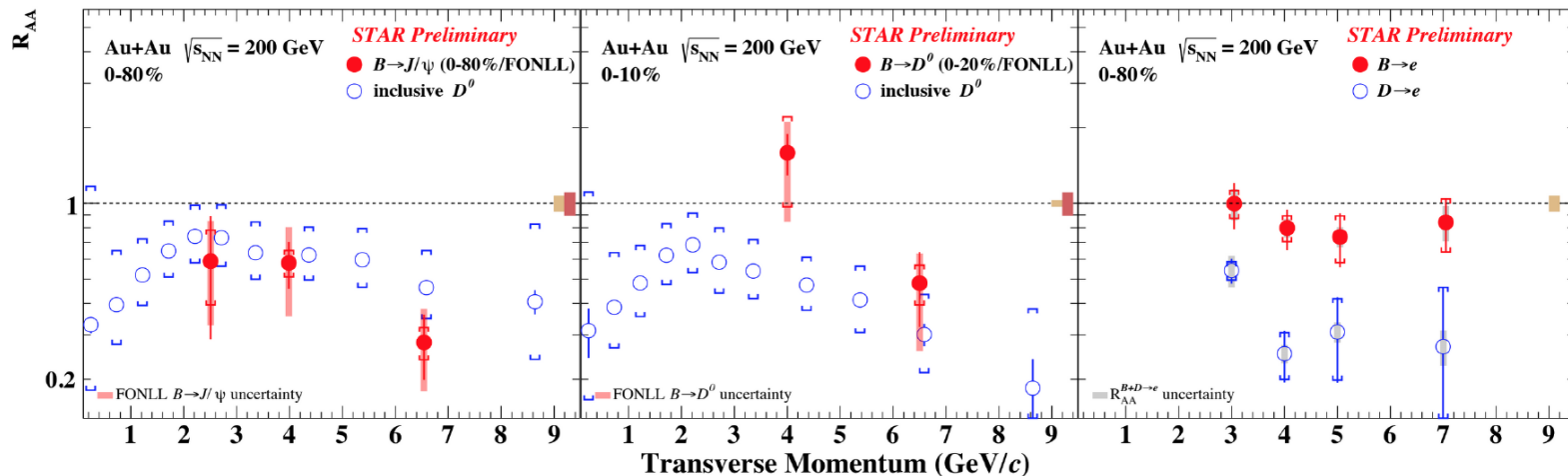


B study from different channels

Strong suppression for $B \rightarrow J/\psi$ and D^0 at high p_T .

Indication of less suppression for $B \rightarrow e$ than $D \rightarrow e$ ($\sim 2 \sigma$): consistent with $\Delta E_c > \Delta E_b$

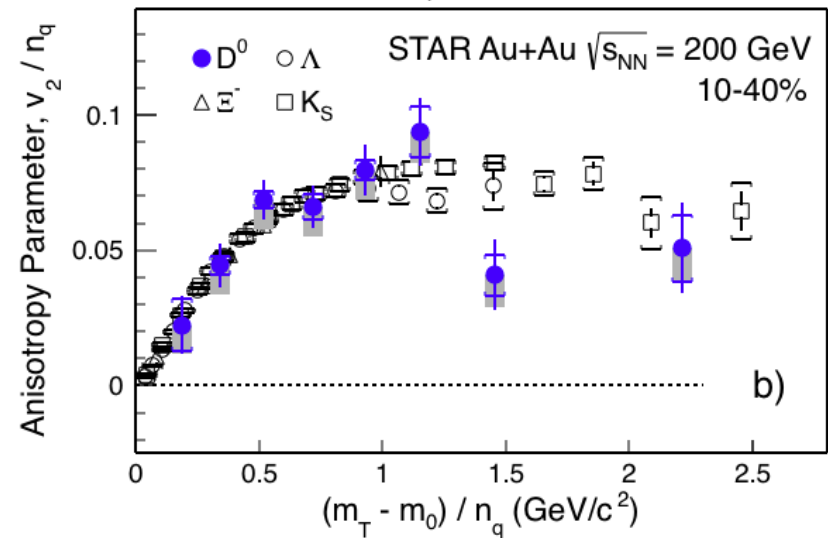
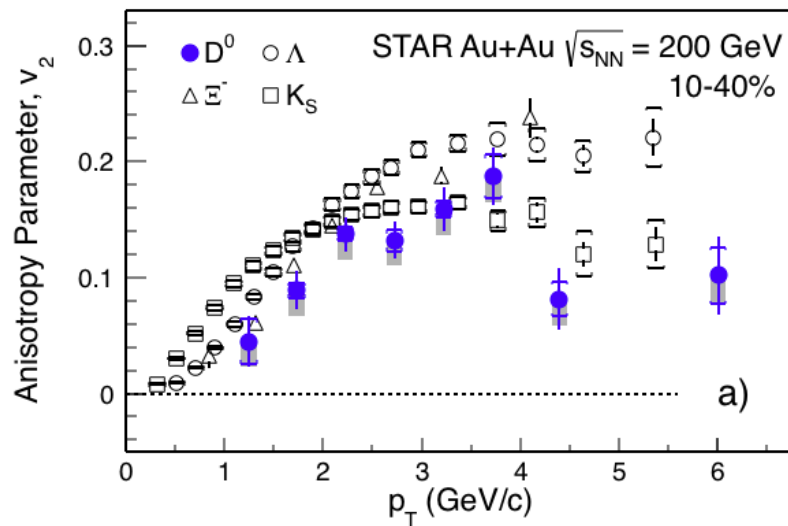
Measurements with improved precision are on the way



Note: R_{AA} references (data vs. theory) are different for these comparisons.
The decay kinematics needs to be unfolded for different channels.

D⁰ Elliptic Flow

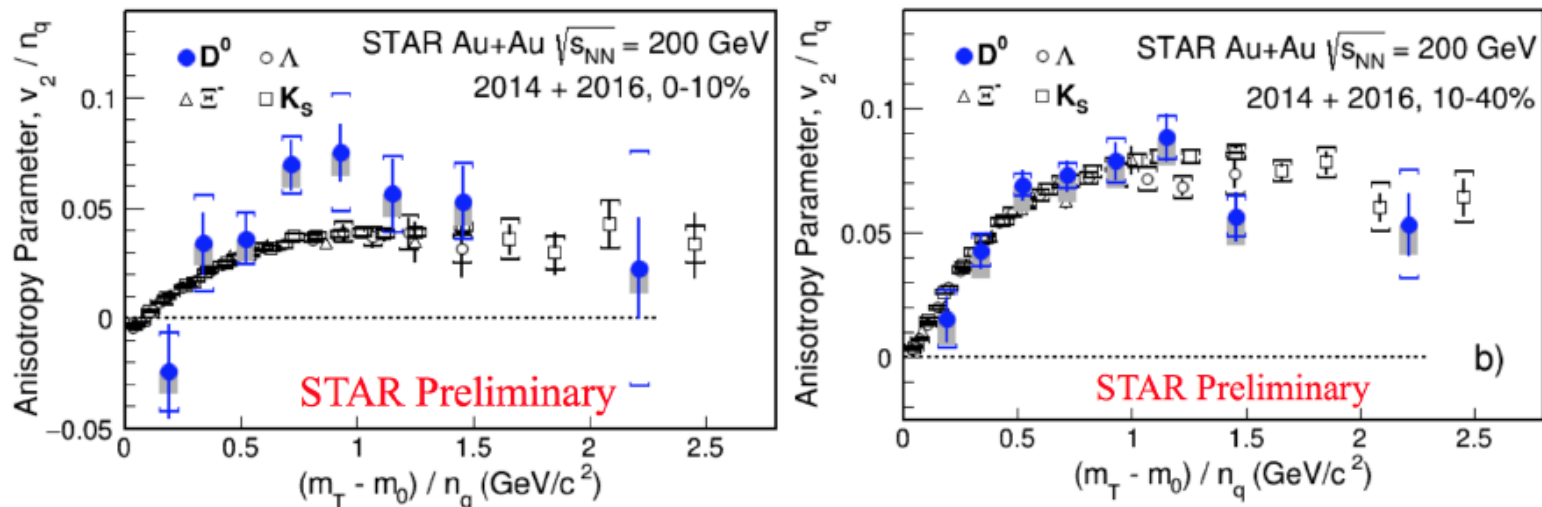
- Published D⁰ v_2 from 2014 dataset
- Clear mass ordering for $p_T < 2$ GeV/c
- Follows NCQ scaling in mid-central (10-40%) collisions



Phys.Rev.Lett 118, 212301 (2017)

D⁰ Elliptic Flow

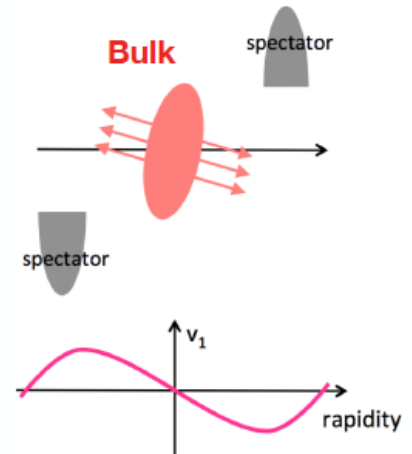
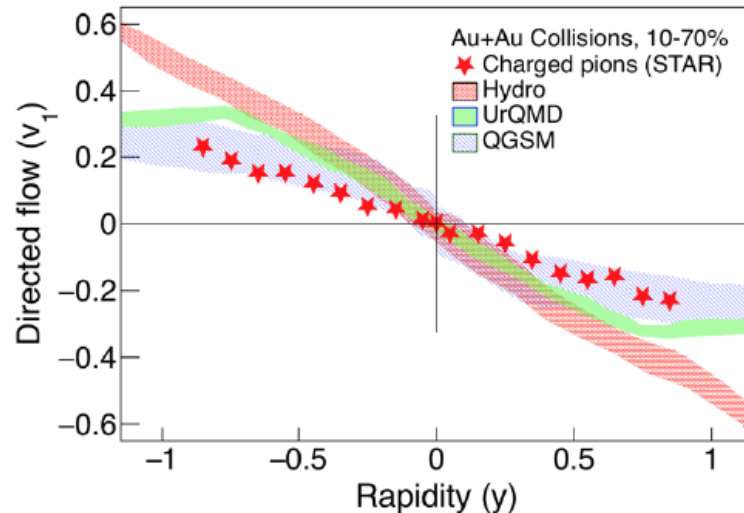
- D⁰ v₂ measurements extended to 0-10% centrality with combined 2014 and 2016 data set
- Significant flow observed



Directed flow in heavy-ion collisions

$$E \frac{d^3 N}{dp^3} = \frac{1}{2\pi} \frac{d^2 N}{p_T dp_T dy} [1 + 2v_1 \cos(\phi - \Psi_R) + 2v_2 \cos 2(\phi - \Psi_R) + \dots]$$

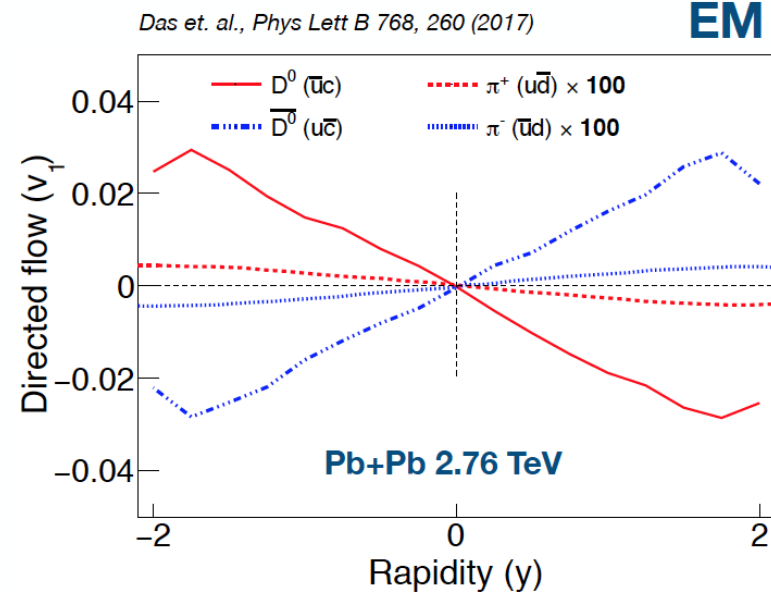
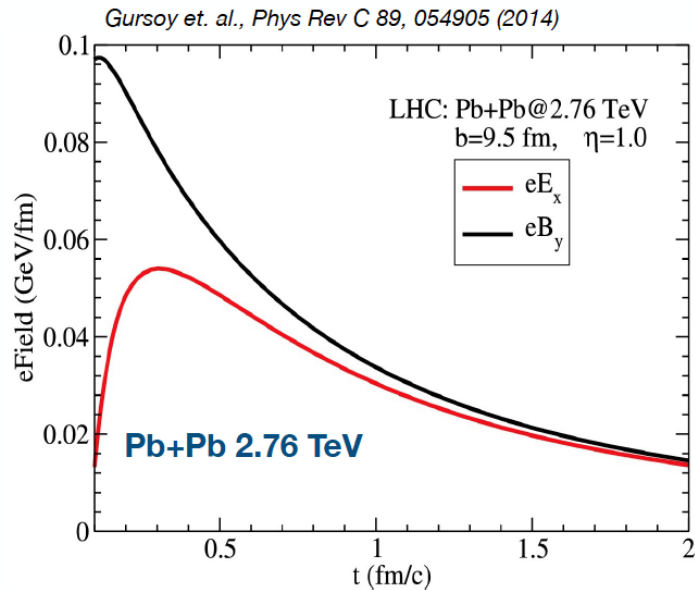
Directed flow $v_1 \sim \langle \cos(\phi - \Psi_R) \rangle$



L. Adamczyk et al. (STAR Collaboration), Phys. Rev. Lett. 108, 202301 (2012)
Hydro: P. Bozek, I. Wyskiel, Phys. Rev. C. 81, 054902 (2010)
UrQMD: H. Petersen et al, Phys. Rev. C. 74, 064908 (2006)
QGSM: J. Beibel et al, Phys. Rev. C. 76, 024912 (2007)
Transport: R. Snellings, et al, Phys. Rev. Lett. 84, 2803 (2000)

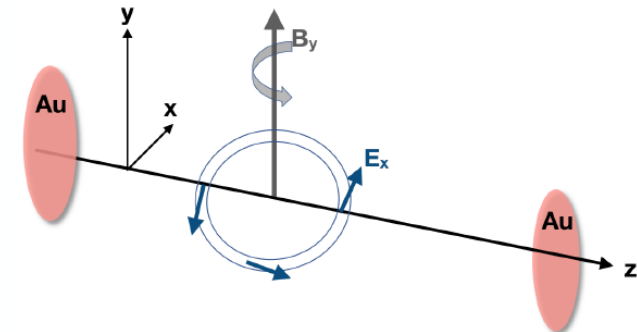
- Charged pions exhibit negative v_1 slope (“anti-flow”) near mid-rapidity
- Models with hadronic physics or with baryon stopping and space momentum correlation can qualitatively explain “anti-flow” shape
- In hydro calculations with initially tilted bulk, the “anti-flow” shape is reproduced
- However, the sensitivity of the charged particle $v_1(y)$ to the tilt parameter is not very strong

Heavy quark v_1 from EM field



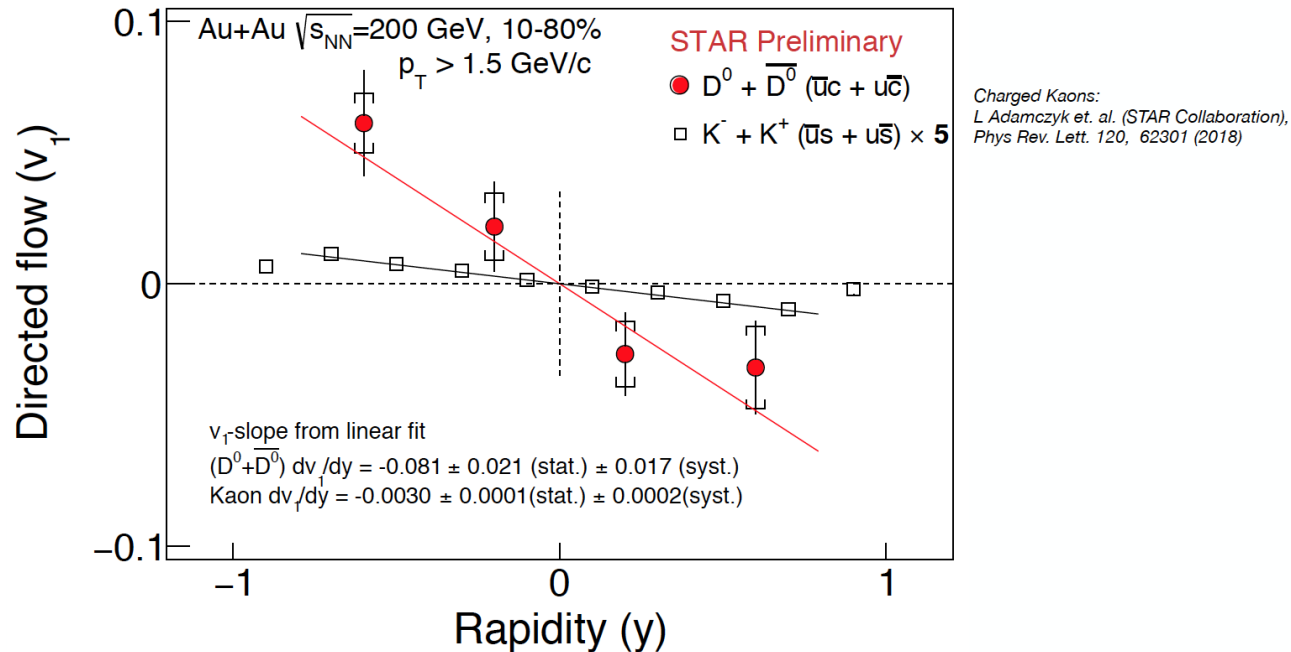
EM

- Incoming charged particles can produce an enormously large EM field
- Due to early production of heavy quarks ($\tau_{cQ} \sim 0.1$ fm/c), positive and negative charm quarks can get deflected by the initial EM force
- Model calculation demonstrates that such initial EM field can induce opposite v_1 for charm and anti-charm quarks
- The magnitude of induced v_1 of charm hadrons can be order of magnitude larger than that of the light flavor hadrons



D^0 and \bar{D}^0 v_1 can offer insight into the early time EM fields

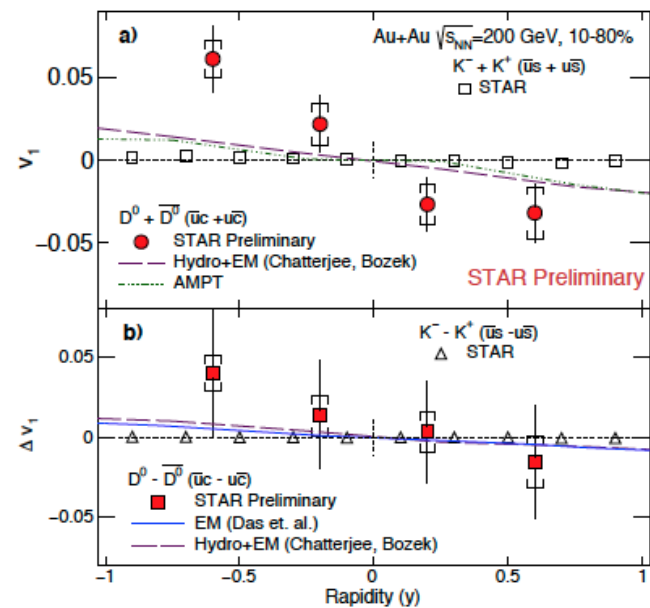
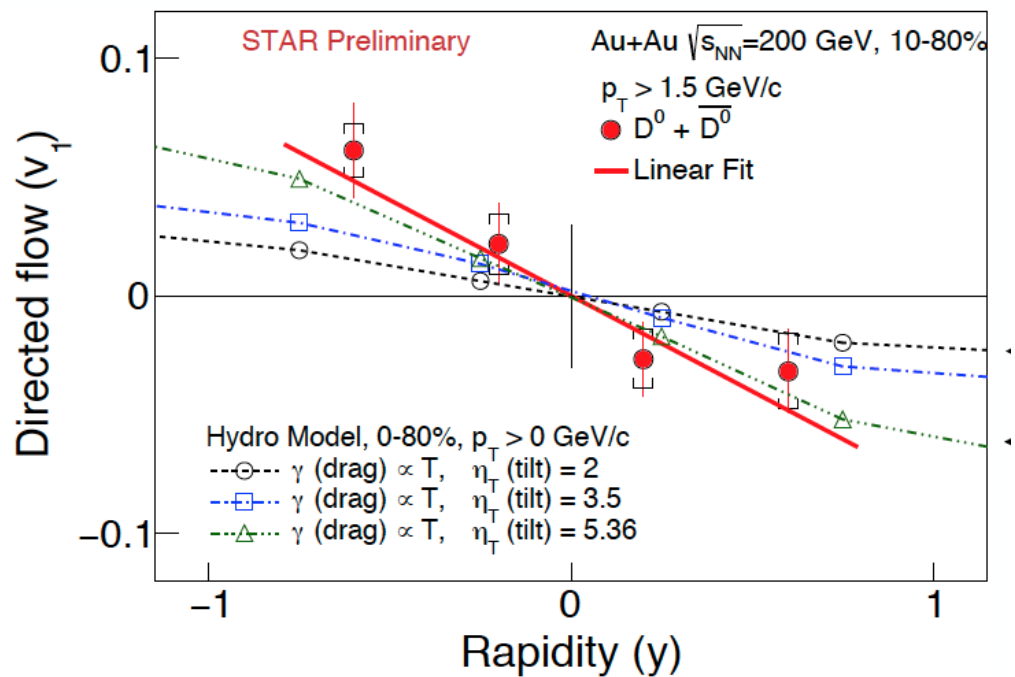
D⁰ directed flow (v_1)



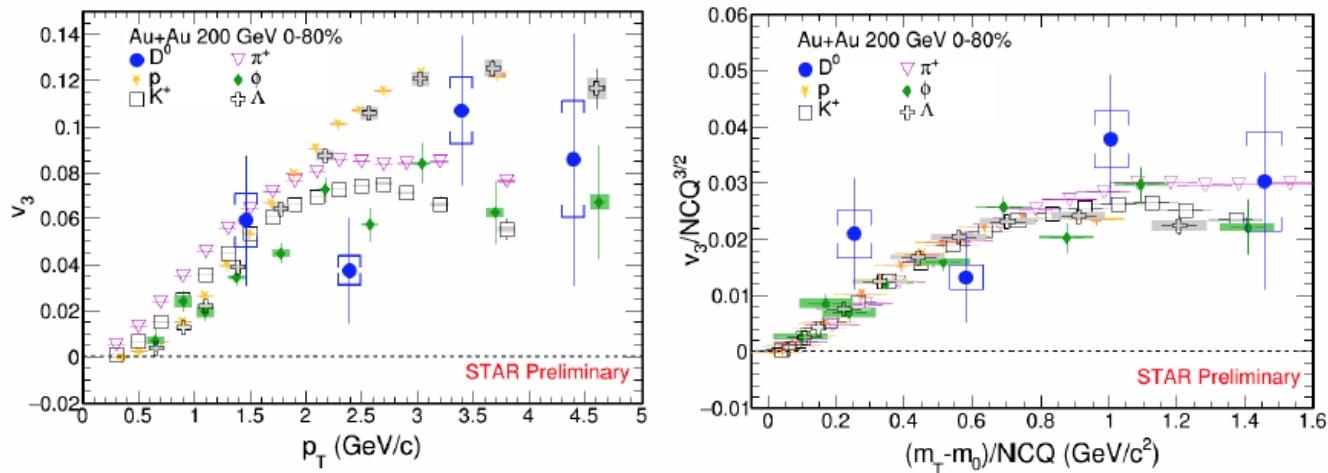
First evidence for non-zero v_1 for D's

Much larger than K^+K^-

May imply effect of strong EM fields in collision system



- ❑ First D^0 v_3 measurement at STAR
- ❑ Large non-zero D^0 v_3
 - ➔ Strong collective behavior
- ❑ Consistent with the NCQ scaling (empirical m_T scaling)
 - ➔ Charm quarks may have acquired similar flow as light quarks
- ❑ Need more statistics to draw a solid conclusion

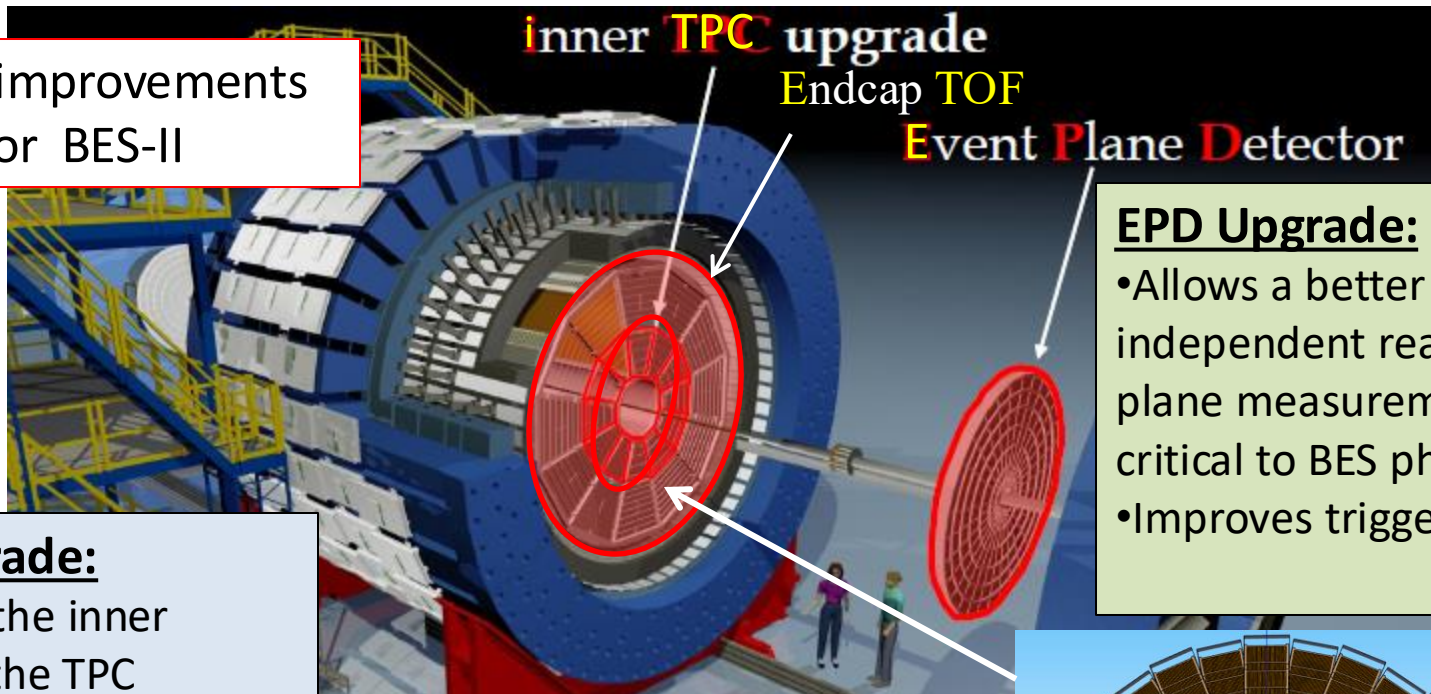


Summary

- The HFT upgrade was overall successfully and has hopefully lead the way for future high resolution vertex detectors (ALICE ITS, sPHENIX, EIC)
- Strong Modification of charm hadron spectra and hadro chemistry in AA collisions as witnessed by the different observations
 - Total charm cross section is conserved.
 - Substantial energy loss , coalescence
 - Gain significant flow & may have achieved thermal equilibrium in medium (v_2)
 - Observed non-zero directed flow
- Indication for suppression at high p_T for $B \rightarrow D^0$,... measurements
- Thanks to the many STAR collaborators that has worked on HFT construction and analysis over the years

The STAR Upgrades and BES Phase II

Major improvements
for BES-II



iTPC Upgrade:

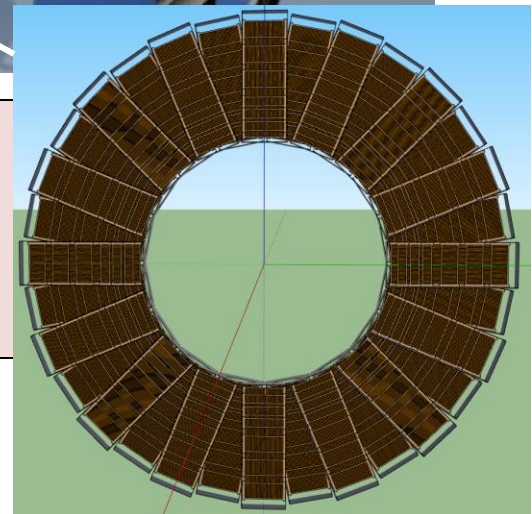
- Rebuilds the inner sectors of the TPC
- Continuous Spatial Coverage
- Improves dE/dx
- Extends η coverage from 1.0 to 1.5
- Lowers p_T cut-in from 125 MeV/c to 60 MeV/c

EndCap TOF Upgrade:

- PID at $\eta = 1.1$ to 1.5
- Provided by CBM-FAIR Phase-0

EPD Upgrade:

- Allows a better and independent reaction plane measurement critical to BES physics
- Improves trigger



All detectors now in place for BES II

